Analysis of the pre-immune T cell repertoire

A DISSERTATION
SUBMITTED TO THE FACULTY OF THE GRADUATE SCHOOL
OF THE UNIVERSITY OF MINNESOTA
BY

Hon Man Hamlet Chu

IN PARTIAL FULFILLMENT OF THE REQUIREMENTS
FOR THE DEGREE OF
DOCTOR OF PHILOSOPHY

Marc K Jenkins, Ph.D., Advisor

DECEMBER 2009

ACKNOWLEDGEMENTS

These four and a half years were very different from what I had expected initially. Nothing really painful, they have been so far the most fun and fruitful years of my life. Every day I learn a little more about science and myself, and I crave for more the next day. I guess my parents would have never expected their only son to become like that. It was really my idea to come to study in the US and they could do nothing but agree, and yet they fulfilled my dream with their unconditional love and endless patience. I know I owe you two forever. Thank you, Mom and Dad.

I lucked out because my life as a graduate student has been perfect. I have an advisor who trusts me enough to let me explore my own interests and direction with his patient guidance and backup. I especially appreciate when you spared your time to listen to me whenever I rushed into your office. Without you I would have never achieved what I did. Thank you for everything, Marc.

If the Jenkins Lab was my second home, then everyone in the lab was a family to me, wherein I would like to make my first heartfelt thanks to James Moon for being such a great partner, mentor and friend. We are the Team Tetramer! Thanks to Jennifer, Kathy, Marion, Traci, Antonio, Drew, James, Jon, Justin, Ryan and everyone else for sharing with me the ups and downs, many conversations, science talks and jokes.

I keep wondering if I could ever find another work place like the Center for Immunology. I do believe that it is one of the most nurturing places for students. Thanks to every member, especially my committee, Kris, Dan, Stephen and Steve for your time, guidance and support.

Being an overseas grad student was not easy. Emotions and stress were inevitable. I am still sane because I have so many great friends to

back me up whenever I need most. Many thanks to all my friends for your warm messages, e-mails, phone calls and caring thoughts. You let me know that I am not alone.

DEDICATION

To

my mother, Wendy and my father, James

ABSTRACT

Cell-mediated immune responses are initiated when a population of pre-immune (or naïve) T cells recognizes their cognate ligands in the form of a specific peptide bound to a self-major histocompatibility complex molecule (pMHC). This recognition is made possible by highly specific T-cell receptors (TCR) on individual T cell clones specific for a given pMHC complex. The pre-immune T cell repertoire is comprised of populations specific for at least 100,000 different pMHC, each containing multiple clones. It is important to understand the composition of this repertoire because it is the repository of the host's potential for future cell-mediated immune responses to microbes and tumors, and in some cases its own tissues. However, the study of individual pre-immune pMHC-specific T cell populations within such a diverse repertoire has been extremely difficult because of their small size.

A novel soluble pMHC-based magnetic enrichment technique was therefore developed to analyze naive T cell populations in mice and humans. Using this procedure, different pMHCII-specific naive CD4+ T cell populations were identified and enumerated. The size of these populations was found to vary depending on pMHC specificity. Additionally, these differences were directly proportional to the magnitude of the primary CD4+ T cell response after immunization with the relevant peptide.Thus, variation in naive T cell frequencies can explain why some peptides give rise to greater T cell responses than others.

We explored this issue by enumerating pMHCII-specific CD4+ T cell populations that normally number 20 or 200 cells per mouse. Thymic positive or negative selection was required for optimizing the absolute size of each population but did not alter the 10-fold ratio between the two

populations. Large naïve population size was related to the presence of certain amino acids at TCR contact sites within the peptide. These results suggest that certain MHCII-bound peptides are immunodominant because they contain amino acids with chemical properties that foster binding to many TCRs.

TABLE OF CONTENTS

LIST OF FIGURES

Page

CHAPTER 3

CHAPTER 4

Page

CHAPTER 5

CHAPTER 1

Introduction

Immunology is the study of how the body's immune system identifies foreign invaders, such as microorganisms and macromolecules, and responds to them. The concept of host defense as a subject of science emerged when smallpox was successfully eradicated by vaccination beginning in 1786. Owing to Edward Jenner and many others, our knowledge of infectious disease pathogenesis led to the birth of modern immunology. From then, the impact of immunology has moved beyond host defense and serves a critical role in the study and treatment of many human diseases.

The primary role of the immune system is defense of the body against infection. Despite much progress towards understanding of host-pathogen interactions and defense mechanisms, the emergence of new and drug resistant pathogens continues to threaten public health. Although vaccines for many infections have been developed to control infections, smallpox is the only human disease that has been eradicated. Understanding the principles of how the immune system functions and interacts with co-evolving microbes remains as a goal for scientists.

The immune system is complex and consists of adaptive and innate arms. The interaction of at least 15 different hematopoietic cell types (not to mention individual clones of lymphocytes) and hundreds of immune cell related surface molecules are involved in these processes. The innate immune system consists of cells (e.g. phagocytes) and molecules (e.g. complement proteins) that become activated by conserved microbe-specific molecules to kill microbes without generating immunological memory. The adaptive immune system consists of lymphocytes each expressing clonally unique antigen receptors, which become activated by microbial antigens to kill microbes and in the process generate long-lived memory cells. Antigen specificity is the central hallmark of adaptive

immunity. The mature lymphocyte pool in a healthy individual contains millions of clones each of which has its own antigen specificity. Detecting, enumerating, and analyzing one naïve antigen-specific lymphocyte population among the hundreds of thousands of others had been difficult. To simplify the problem, transgenic mice containing monoclonal lymphocytes with a single antigen specificity have been generated. Complemented by flow cytometry and sophisticated *in situ* imaging, this reductionist approach advanced knowledge in most aspects of T cell biology for the past decade. However, the artificiality of this monoclonal approach has prevented further understanding of the complexity in the normal polyclonal T cell repertoire and the responses derived from it *in vivo*. This missing information may be a key for developing treatments against infections, cancers and autoimmune diseases in humans.

My thesis project was to develop a system that made it possible to isolate, enumerate and analyze very rare pMHC-specific naïve T lymphocyte populations in the polyclonal repertoires of normal humans and mice. This methodology enabled us, for the first time, to provide information on the composition of the pre-immune T cell repertoire and the mechanism of immunodominance.

BACKGROUND AND SIGNIFICANCE

The Clonal Selection Theory of Acquired Immunity

The knowledge of microorganisms as infectious agents that can elicit an immune response and cause diseases was not introduced until a century after the success of smallpox vaccination. These findings allowed Louis Pasteur to formulate new vaccines against other diseases such as rabies in the 1880s (1). Since then the quest for the mechanisms of

protection from infection has intensified. In the early 1890s, the identification and isolation of antitoxin (antibody) in the serum of animals immune to diptheria toxin by Von Behring and Kitasato provided the basis of humoral immunity (2). Along those lines, Paul Ehrlich observed that a vast amount of antibody could be produced upon primary exposure to an antigen in the blood (3). He proposed the side-chain theory (4), which posited that surface receptors on blood cells were capable of recognizing all naturally occurring antigens and that the binding of antigen induces the release of the receptors as antibodies.

However, several important features of acquired immunity were not explained by the side-chain theory: 1) exponential production of antibodies after primary exposure to antigen; 2) antibodies can be found long after antigen is cleared from the body; 3) secondary exposure to the same antigen elicits improved production and fitness of the antibodies (2 & 3 are features of immunological memory); and 4) antibodies can be made against virtually any foreign antigen but not against host-derived proteins.

Jerne adopted the previous theories and features of the adaptive immunity to propose the “natural selection theory” (5). He argued that a small repertoire of randomly generated antibodies exist before the encounter with antigen. Antigen “selects” one of the pre-existing antibodies of high affinity and leads to production of more antibodies with the same specificity. Antibodies against self-antigens are eliminated before damaging the host by unknown mechanisms. However, using antibody molecules as the basic recognition unit of the system could not explain how the antigen-selected antibodies replicate on their own.

In the 1950s, David Talmage and, most importantly, F. Macfarlane Burnet, extended Jerne’s theory by introducing “cells” as the basic unit of the antigen-antibody selection mechanism (6). Burnet’s “clonal selection

hypothesis of antibody diversity" suggests that in a repertoire of millions of immunocompetent cells, each randomly express on their surface an antigen receptor of unique specificity prior to exposure to any antigen. Cells that by chance express a self-reactive receptor will be deleted during an immature stage of developmental. Following exposure to antigen, rare clones with the best matching receptor bind the antigen and proliferate. Antibodies of the same specificity as the receptor are produced by the clonally expanded cells, which can explain the exponential increase of antibody quantity after primary immunization.

After more than 50 years of experimental proofs, the clonal selection theory has become the framework for studying the adaptive immune responses of higher vertebrates. Although the innate immune system is a critical first line of defense against pathogen invasion and detection of microbial products, the adaptive arm of the immune system provides highly specific, rapid and long-term protection from future infections with similar pathogens.

Basis for antigen specificity and diversity in adaptive immune responses

Antibodies were the first component of the adaptive immune system to be identified, due to their appearance in extracellular fluids in significant quantities after immunization. Their high degree of specificity against virtually any foreign antigen led to the idea that antibodies were the basic unit of the adaptive immune system. However, based on the influence of the clonal selection theory, James Gowans confirmed that small lymphocytes are the functional units of adaptive immunity and immunological memory (7). Shortly thereafter, two classes of antigen-specific lymphocytes, namely B and T cells were discovered as

determinants of antigen specificity and functional mediators in the adaptive immune system (8, 9). B cells, which are produced in the bone marrow, are responsible for antibody secretion to activate the complement cascade and provide toxin neutralization (9). T cells, which are derived from the thymus, are responsible for allograft rejection, helping B cells to secret different classes of antibodies, lysis of infected cells, and activation of innate immune cells such as macrophages (10, 11).

Different classes of antibodies, which exist either in the form of membrane-bound surface receptors, or in secreted form, determine the specific antigen recognition of B cells. The equivalent antigen recognition receptor on T cells is the T-cell antigen receptor (TCR), which only exists in membrane-bound form. The observation that the immune system can recognize a seemingly unlimited array of antigens suggests an enormous diversity of antigen receptors in the T and B lymphocyte pools. Based on the pioneering studies of Susumu Tonegawa (12), it is now known that the genes encoding lymphocyte antigen receptors are produced by somatic recombination of the variable (V), diversity (D) and joining (J) gene segments at the *Tcr* or *Ig* loci. This recombination process occurs during the development of lymphocytes and is mediated by a specific enzyme encoded by the *recombinase activating* (*RAG*) genes (13). Somatic recombination is essential to antigen receptor diversity because it is capable of generating as many as 10^{15} unique receptors from a small set of genes (14). This vast diversity is a combination of the rearrangement of the V(D)J gene segments and non-templated sequences that are randomly added at the sites of gene recombination. The vast number of possible antigen receptor rearrangements makes it likely that each clone in the repertoire carries a unique antigen specificity.

T cell recognition of pMHC ligands

The antigen receptor determines the specificity of T and B lymphocytes. How these antigen receptors recognize their ligands is therefore a critical subject in understanding the adaptive immune system. Unlike B cell antigen receptors, or antibodies, which bind to macromolecules based on their confirmation, T cells do not respond to soluble antigens but only to foreign peptides on the surface of other immune cells from the same individual. The T cell response depends on products of the polymorphic *Immune response* (*Ir*) genes encoded in the major histocompatibility complex (MHC) (15). The basis of the T cell response was demonstrated unequivocally by Zinkernagel and Doherty when they showed that virus-specific T cells would kill virus-infected target cells only if they expressed the same MHC molecules as the strain from which those T cells developed (16). Further studies showed that foreign protein antigens are displayed on the surface of antigen presenting cells in the form of 8 – 20 amino acid long peptide fragments embedded in the peptide binding groove of a MHC molecule (17-19). Thus, antigen recognition by T cells is restricted to self-MHC molecules with the cognate peptide ligand in the binding groove.

The peptide display function of MHC molecules and T cell recognition and activation based on that presentation provides the basis of cell-mediated immunity. The surface display of peptide-MHC complexes (pMHC) by antigen presenting cells allows the immune system to identify cells that harbor intracellular antigens or microbes. Among the different classes of lymphocytes, CD4+ T cells play a pivotal role in the adaptive immune system by stimulating antibody production in B cells and helping CD8+ T cells to better kill infected cells and achieve immunological memory (20).

The details of MHC structure and function in antigen presentation have been studied extensively since the discovery of MHC-restricted recognition by T cells. Two classes of MHC molecules, MHC class I (MHCI) and class II (MHCII) display peptides derived from different cellular compartments due to distinct mechanisms of their intracellular assembly and transport (21). Traditionally, MHCI molecules present peptide fragments from intracellular or cytosolic proteins to CD8+ T cells, while MHCII molecules present extracellular or vesicular protein fragments to CD4+ T cells. However, recent studies show that antigen presentation by MHCI and MHCII are not limited to the location of the proteins. In certain cells, MHCI can process and present extracellular antigens by a mechanism known as cross-presentation (22). On the contrary, MHCII can present intracellular antigens by autophagy (23). It has been established that each MHCII-bound peptide has 9 core amino acid residues. Side chains of amino acid position 1, 4, 7 and 9 are buried in the MHCII groove to promote MHC binding, while side chains of amino acids at position 2, 3, 5 and 8 point upwards and interact with the TCR (24). This structural feature of an MHCII-bound peptide is conserved among different classes and allelic forms of MHCII molecules across higher vertebrate species.

The paradigm of MHC restricted recognition by T cells has led to many important discoveries about TCR recognition of antigen (25, 26). It is now known that the TCRs are heterodimers comprised of α- and β-chains or γ- and δ-chains. The α- and γ-chains contain V and J regions while the β- and δ-chains contain V, D, and J regions. My thesis focuses on T cells that express $\alpha\beta$TCRs, which are much more abundant than $\gamma\delta$T cells. Through many studies of $\alpha\beta$TCR:pMHC crystal structures, it is now known that these TCRs bind to pMHC complexes via their complementary-determining region (CDR) loops: CDR1α, CDR2α, CDR1β, CDR2β in the

V-region, and CDR3α and CDR3β at the junction region between Vα and Jα or Vβ and Dβ/Jβ, respectively. These six CDR loops contact the surface of pMHC. CDR1α and CDR2α often interact with the α2 helix of the MHCI or β helix of MHCII, and CDR1β and CDR2β interact with the α1 helix of the MHCI or α helix of MHCII. In contrast, the CDR3α and CDR3β primarily interact with the amino acid side chains of the peptide bound in the MHC groove. It is now known that the germline-encoded CDR1 and CDR2 loops are predisposed to interact with certain amino acids on MHC helices (27). These interactions are thought to impose the diagonal conformation of TCR binding on the MHC molecules. Such topology could allow the hyper-variable CDR3 loops in contact peptides of different amino acid sequence and length, which defines the fine specificity of the TCR:pMHC interaction.

The binding of TCR to pMHC is aided by the CD4 or CD8 co-receptors (24). The CD8 molecules expressed on CD8+ T cells facilitate binding to the invariant α3 region of the MHCI molecules, while the CD4 molecules expressed on CD4+ T cells have affinity for the invariant β2 domain of MHCII molecules. Moreover, these co-receptors are critical to initiate signals immediately after TCR:pMHC interaction (28). CD4+ and CD8+ T cells express the appropriate class of co-receptor that matches their TCR specificity to MHCII or MHCI.

Thymic selection of the pre-immune MHC-restricted T cell repertoire

The pre-immune T cell pool consists of millions of T cells each expressing a TCR with a unique pMHC specificity. If the generation of a diverse TCR repertoire is due to a random recombination process, the chance of clones with no pMHC specificity or with self-antigen reactivity is inevitable. How then does the pre-immune T cell repertoire only contain

foreign-reactive T cells but not self-reactive ones? The key lies in the thymus, where T cell development occurs.

T cell progenitors derived from bone marrow hematopoietic stem cells travel to the thymus for a series of developmental processes before populating the secondary lymphoid organs. Upon arriving in the cortex of the thymus, T cell progenitors must produce in-frame TCRβ and TCRα chains by V(D)J gene rearrangement in order to commit to the $\alpha\beta$ T cell lineage. These recombination events occur at the CD4+ CD8+ stage of development. TCR recognition of MHC molecules is essential for T cell maturation and differentiation because loss of both MHCI and MHCII molecules results in the arrest of T cell development at the CD4+ CD8+ stage (29). Collective efforts from many studies determined that T cell maturation from the CD4+ CD8+ stage is the outcome of two selection events governed by self-pMHC complexes expressed in the thymus (30).

The CD4+ CD8+ thymocytes interact with radio-resistant cortical thymic epithelial cells in a process known as positive selection (31). Only clones with TCRs of low affinity for self-pMHC receive survival signals to further differentiate (32, 33). Clones with negligible self-pMHC affinity will die by neglect. Recent identification of self-peptides for particular MHCI- and MHCII-specific TCRs indicates that self-pMHC conformation is critical for positive selection of thymocytes (34-36). Each TCR has a limited set of self-pMHCs that are in the affinity range needed for positive selection (33).

Another function of thymic positive selection is to instruct CD4+ CD8+ thymocyte differentiation into either the CD8+ cytotoxic T cell lineage or the CD4+ helper T cell lineage (37). If a TCR is specific for a particular self-pMHCI with low affinity, the clone will become a CD8 T cell; on the contrary, if a TCR is specific for a self-pMHCII with a slightly higher affinity, this clone will become a CD4+ T cell. The specific TCR-pMHCI-

CD8 interaction or the TCR-pMHCII-CD4 interaction induces the upregulation of the master regulator gene Runx3 or ThPOK respectively for CD8+ or CD4+ lineage stabilization (38-40).

Upon receiving survival signals in the cortex, the positively selected thymocytes spend the next 4-5 days in the medulla (41) They increase their migration velocity to maximize the interaction with medullary thymic epithelial cells (mTECs) and thymic dendritic cells (DCs) (42). The mTECs express self-pMHC complexes under the control of a transcription factor called autoimmune regulator (AIRE), which allows the expression of a diverse arrays of tissue-specific antigens that are not normally found in the thymus (43, 44). Recent data also suggest that unidirectional transfer of self-antigens from mTECs to thymic dendritic cells is a constant process and is important for the process of negative selection or clonal deletion (45).

Highly self-pMHC-reactive T cell clones are present in the positively selected population (46). Their TCRs are of high affinity for MHC with peptide derived from self-antigens, and could cause autoimmune diseases if they migrate to the secondary lymphoid organs. Through the interaction with thymic DCs or mTECs, clones with TCRs capable of binding to self-pMHC with high affinity undergo apoptosis or may become T regulatory cells through poorly understood mechanisms. Mice with acute depletion of T regulatory cells develop organ-specific autoimmune diseases suggesting the presence of self-reactive T cells in the pre-immune T cell repertoire as well as incomplete thymus-induced tolerance (47). Several studies have pointed out that self-reactive T cells in the pre-immune repertoire are of low affinity, which might be the reason why they can escape negative selection (48, 49). However, T cells expressing TCRs with a high enough

affinity for self-pMHC to cause autoimmunity have yet to be detected directly *ex vivo*.

Cell-mediated immunity and functional consequences of T cell repertoire diversity

During infection, pathogens invade the host by penetrating barrier surfaces, such as the skin or mucosa. At the site of infection, epithelial cells and other tissue-resident innate immune cells such as DCs and macrophages sense microbial products released by pathogens via pattern recognition receptors (PRRs) such as toll-like receptors (TLRs) (50). Engagement of TLRs activates secretion of inflammatory cytokines and chemokines for phagocyte recruitment. Although the innate inflammatory response provides immediate control of infections, this control is limited and does not produce immunological memory. Moreover, prolonged inflammation is harmful to the host due to tissue necrosis and the potential of autoimmunity. Adaptive immunity is thus needed to clear the infection and provide future protection to the same infection.

Tissue-resident dendritic cells (DCs) play a key role in initiating the adaptive T cell response. These cells pick up pathogens or microbial antigens at the site of inflammation and migrate to the site-draining secondary lymphoid organs, such as lymph nodes and mucosa-associated lymphoid tissues via afferent lymphatic vessels (51, 52). When arriving in the secondary lymphoid organs, the DCs enter the T-cell areas where naive T cells reside. At the same time, the DCs process the microbial antigens and display an array of microbe-specific peptide fragments in the context of MHC molecules on the surface (21).

Due to the diversity of the pre-immune T cell repertoire, the number of T cells specific for a single microbial pMHC in a particular lymph node is

rare. How then do these rare T cells encounter these pMHC presented by the DCs in the lymph nodes? Naive T cells recirculate through the secondary lymphoid organs via the blood, spending about 6 hours in each organ. Their relatively high velocity in the T-cell area of the secondary lymphoid organs maximizes their chance to sample pMHC presented on many different DC surfaces (53). Once a rare naïve T cell finds the microbial pMHC for which its TCR is specific, it forms a stable contact with the DC for the next 8-24 hours in order to become activated (54). This is followed by rapid proliferation and differentiation of that T cell.

At least two signals are required for complete CD4+ T cell activation (55). Signal one is initiated by the TCR upon binding to the cognate pMHC. Signal two is a co-stimulatory signal from CD28:CD80/86 ligation. The homodimeric molecule CD28 is constitutively expressed on the T cell surface, while CD80 and CD86 molecules are expressed at a basal level on DCs and other cells during non-inflammatory conditions, but are highly upregulated upon activation via TLR engagement or inflammatory cytokines such as IL-1, TNF-α or IFN-γ (56). Many studies have shown that the CD28 co-stimulatory signal is essential for maximal clonal expansion of T cells. Both *in vitro* and *in vivo* studies demonstrated that TCR ligation without signal two induces T cell unresponsiveness (also called T cell anergy (57-59)). Since the Clonal Selection Theory predicts that clonal expansion of rare naïve pMHC-specific T cells is the basis for T cell immunity, it is not suprising that effective immunization depends on adjuvants that induce CD28 ligands.

Although the co-stimulatory signal dictates T cell proliferation, the quality of the TCR signal has also been suggested to be a determinant of T cell effector function. The polyclonal T cell repertoire contains individual clones expressing TCRs with a spectrum of affinities for a given pMHC.

The affinity of a TCR for its ligand is known to correlate with the quality of downstream signaling. For example, Malherbe et al. (60) proposed that there are two TCR affinity thresholds regulating CD4+ T cell activation. The first low threshold allows initial recruitment of high and low affinity T cells into the early stage of the immune response. The second threshold selects only high affinity clones for the effector and memory phases of the response. Similarly, Zehn et al.(61) showed that low affinity, microbe-specific T cells can proliferate early after infection but high affinity clones, due to their sustained proliferation, eventually dominated the overall T cell response. This line of evidence suggests that memory T cells are generated from high affinity clones. Teixeiro et al. (62) supported this idea by demonstrating that diminished TCR signaling by genetic mutation of TCR β chain reduced T cell memory formation but not initial clonal expansion.

TCR affinity has also been suggested to regulate T cell effector function. McHeyzer-Williams and colleagues demonstrated that high affinity CD4+ T cells tend to differentiate into T-follicular helper cells (63), which support B-cell receptor somatic hypermutation in the germinal centers. On the other hand, other groups including Paul and colleagues proposed that high affinity T cells are likely to differentiate into Th1 cells, while low affinity T cells are prone to become Th2 cells (64, 65). Th1 cells upregulate the transcription factor T-bet (66) and primarily secrete IFN-γ to help clear intracellular pathogens (67); Th-2 cells upregulate the transcription factor GATA-3 and secrete IL-4, 5 and 13, which help to mediate clearance of extracellular pathogens (68). Moreover, recent reports have shown that optimal TCR affinity is also crucial for cytotoxic granule delivery in both CD4+ and CD8+ T cells (69, 70). It is therefore

clear that a diverse TCR repertoire ensures T cell functional heterogeneity for optimal immune response against infections.

Immunodominance in the T cell response against infections

Although many pMHC are derived from pathogens during infection, the T cell responseis often directed against a small number of these pMHC (71). The cause of this phenomenon, known as immunodominance, is largely unknown. Understanding the mechanism is fundamental to the development of cellular-based vaccines and immunotherapy. Many years of effort have been made to determine the factors causing this immunodominance hierarchy. Some studies pointed to a role for antigen dose, location, and expression pattern; antigen processing and presentation; and peptide affinity for MHC molecules (72). However, studies of immunodominance have relied almost exclusively on CD8+ T cell-mediated immunity in several viral infection models. The role of immunodominance and its determinants in CD4+ T cell-mediated immunity remain elusive.

The size of naïve foreign pMHC-specific T cell populations available in the repertoire could also be a major factor in immunodominance. However, current technology limits our ability to enumerate and isolate the exceedingly rare foreign-pMHC-specific T cells directly from a normal T cell repertoire. Development of a novel tool was necessary for this purpose.

EXPERIMENTAL APPROACH

The adaptive immune system is complex as its functions depend on interactions between many different cell types at different locations. Understanding lymphocyte responses *in vivo* is particularly challenging because each lymphocyte has a unique antigen specificity. Tracking the migration and response of any given antigen-specific lymphocyte population during the course of an immune response is a “needle in the haystack” problem. Therefore, immunologists have developed several reductionist systems to minimize the frequency problem as much as possible.

Most, if not all, of the studies in the early years were done in *in vitro*. Bulk lymphoid cells freshly isolated from mice or humans were cultured in a dish and provided with exogenous stimuli such as antigens and cytokines. The whole culture would then be subjected to proliferative or cytotoxic activity measurement (16, 73). It was soon realized, however, that *in vitro* assays could not represent the T cell response *in vivo*, and that responses by naïve pMHC-specific T cells were undetectable by this approach. Thus, the activity of antigen-specific T cells could only be measured from expanded populations, which were often generated through repeated antigen stimulation and thus possibly not reflective of the state of the initial naïve pool (74).

TCR transgenic mice and the adoptive transfer system

The advent of TCR transgenic mice allowed the study of naïve antigen-specific T cells during the primary response *in vivo.* Forcing transgenic expression of a particular $\alpha\beta$ *Tcr* gene combination in the T cell lineage during thymocyte development generates TCR transgenic mice

(75). By crossing the *Tcr* transgenes onto the RAG-1- or RAG-2-deficient background, mice are produced that contain a monoclonal T cell population specific for a defined pMHC. To date, several dozen CR transgenic mouse strains are available as a source of naïve T cells with a single, defined pMHC specificity.

It is important to note that the lymphoid system in TCR transgenic mice is abnormal due to the lack of B cells and T cells with other specificities. Therefore, these animals are not an ideal physiological host for *in vivo* studies. The Jenkins laboratory revolutionized the field by developing the approach of transferring a few million naïve TCR transgenic T cells into unmanipulated MHC-matched host mice followed by immunization with the relevant antigen (58, 76). The host mice express an allelic form of the surface proteins CD45 or CD90 that allows the donor cells to be distinguished from the host T cells by using antibodies specific for these allelic markers. This adoptive transfer system allows the tracking of numbers, phenotypic changes, and location of the donor pMHC-specific T cells during the course of an immune response *in vivo*.

A major caveat of this approach has recently come to light in that the number of donor TCR transgenic T cells transferred far exceeds the naive frequency of T cells with the same specificity in normal mice. The competition for pMHC among the transgenic T cells is artificially increased leading to inhibition of activation and memory cell generation (77, 78). Adjusting the number of donor T cells down to the endogenous level can solve this problem. The detection sensitivity of the relatively small number of cells in the host is enabled by the magnetic bead-based enrichment method described below (79).

Another problem associated with TCR transgenic T cells is that every donor T cell expresses the same TCR with a fixed affinity for pMHC.

The use of a monoclonal population thus prevents the study of repertoire diversity, immunodominance, and affinity-based cell fate determination of pMHC-specific T cells. A method was needed for the direct isolation, characterization and quantification of endogenous pMHC-specific T cell populations in a polyclonal repertoire. The invention of soluble pMHC multimer technology provided this opportunity.

Enrichment of pMHC-specific naïve T cells from a polyclonal repertoire by soluble pMHC multimers

The pMHC tetramer as a new class of T cell detection reagent was developed two years after the first report of the adoptive transfer system (80). Soluble mouse or human biotinlyated MHCI or MHCII molecules with foreign peptides bound in their grooves are expressed and purified. The pMHC monomers are then conjugated to a streptavidin-labeled fluorochrome to produce pMHC tetramers (80, 81). These tetramers can bind to T cells expressing the cognate TCR. The high avidity of pMHC tetramers compensates for the low affinity of pMHC:TCR interactions and provides stable binding with T cells. There are two major advantages of using pMHC tetramers over the adoptive transfer system to study the T cell immune response. First, virtually any pMHC-specific T cell population can be analyzed in any genetic background because the detection is solely dependent on pMHC tetramers. Soluble pMHC complexes can be synthesized with any peptide specificity bound to any MHC molecule, as long as the amino acid sequence is known. Second, detection of pMHC-specific T cells can be performed without the use of monoclonal TCR transgenic T cells. The method permits the analysis of the endogenous T cell response at the most physiological level, as well as analysis of human samples.

However, the use of pMHC tetramers was still limited by the low frequency of pMHC-specific T cells. Accompanying tetramer staining with magnetic bead-based enrichment solved this problem. This method opened the opportunity for analyzing T cell responses to infectious agents, tumors, or autoantigens in an unbiased fashion.

STATEMENT OF THESIS

This thesis describes a system that allows, for the first time, the visualization of pre-immune foreign pMHC-specific T cell population dynamics and responses from the polyclonal repertoire in mice and humans. The principle hypothesis is that the sizes of naïve T cell populations vary with their pMHC specificities, and the size differences among populations can explain the phenomenon of immunodominance. We also hypothesize that the size of a pMHC-specific T cell population is determined by thymic selection and the properties of TCR contact residues in pMHCs.

CHAPTER 2

Materials and Methods

Mice

Six-8 week old C57BL/6 (B6), BALB/c, C.B10-*H2*^{b}, B6.C-*H2*^{d}, FVB, (B6 x BALB/c) F_1 mice were purchased from the National Cancer Institute or The Jackson Laboratory. B6 *Rag-1-/-*, B6 *Cd90.1*+, SM1 *Rag-1-/-,* DO11.10 *Rag-1-/-*, OT-II *Rag-1-/-,* TEa *Rag-1-/-,* and YAe mice were bred in our facilities. *H2-DMa-/-*, K14-*A*$^{b}\beta$*-/-*, *JH-/-*, μMT and NOD mice were kindly provided by A. Rudensky (Memorial Sloan-Kettering Cancer Center), T. Laufer (University of Pennsylvannia), W. Weidanz (University of Wisconsin), M. Farrar and B. Fife (University of Minnesota), respectively. All mice were housed under specific pathogen-free conditions in accordance with University of Minnesota and NIH guidelines.

Bone marrow chimeras

T-cell depleted bone marrow cells obtained from (B6 x BALB/c) F_1 mice were injected intravenously into lethally irradiated (1,000 rads) B6 or BALB/c mice. Similarly, lethally irradiated B6, *H2-DMa-/-* or YAe mice were reconstituted with T-cell depleted bone marrow cells from B6, *H2-DMa-/-* or YAe mice. Chimeras were used for experiments 8 to 12 weeks after bone marrow transfer.

Antibodies and peptides

Fluorochrome-labeled antibodies specific for murine or human molecules were purchased from eBioscience, Caltag, or BD PharMingen. All peptides were purchased from GenScript Corporation except the influenza A virus hemagglutinin 307-319 peptide (AnaSpec).

Immunization

Mice were injected intravenously with 50, 1, or 0.1 µg of indicated peptides with 5 µg of LPS (List Biologicals) or 2 x 10^6 T-cell depleted (B6 x BALB/c) F_1 splenocytes that were first incubated with 100 µg/ml 2W1S peptide at 37^{o}C for 2 hours. Human subjects received the inactivated influenza vaccine containing an H3N2 A virus, an H1N1 A virus, and a B virus via intramuscular injection.

Plasmid construction

pRMHa-3 vectors containing the alpha and beta chains of I-A^d under the control of the metallothionein promoter were provided by N. Glaichenhaus (82). These constructs included C-terminal fusions to acidic and basic leucine zipper domains to force heterodimerization (83), as well as a 6x His epitope tag on the beta chain construct to facilitate purification, and an IgG2a-Fc domain on the alpha chain. The I-A^d sequences in both constructs were replaced with corresponding I-A^b alpha and beta sequences generated by PCR amplification. The Fc domain on the alpha chain was replaced with a BirA biotinylation signal sequence (84) generated by oligonucleotide synthesis. Sequences encoding antigenic peptides (FliC 427-441: VQNRFNSAITNLGNT, $FliC_{1W}$: VQNRFWSAITNLGNT, $FliC_{2W}$: VQNRFWSAITNWGNT, 2W1S: EAWGALANWAVDSA, 3K: EAQKALANKAVDKA, 1R: EARGALANWAVDSA, 1G: EAGGALANWAVDSA, OVA 323-339: ISQAVHAAHAEINEAGR, IgM heavy chain 376-391: EKYVTSAPMPEPGAPG) were fused to the N-terminus of the beta chain via a flexible polyglycine linker (85). The constructs encoding OVAC and $OVAC_{1W}$ molecules were generated by mutating the valine residue at the I-A^b alpha chain position 72 to cysteine. Sequences encoding antigenic peptides were (OVAC: HAAHAEINEAGC, $OVAC_{1W}$: HAWHAEINEAGC). A

similar approach was used to produce soluble HA:DR4 molecules. A pRMHa-3 vector was constructed to encode the DRA*0101 chain followed by an acidic leucine zipper and a BirA biotinylation signal sequence at the C-terminus. A separate pRMHa-3 vector was constructed to encode the influenza A virus hemagglutinin 307-319 peptide (PYKVKQNTLKLAT) (86) fused to DRB1*0401 by a flexible polyglycine linker followed by a basic leucine zipper and a His epitope tag at the C-terminus.

Peptide:MHCII tetramer production

Peptide:I-A^b or HA:DR4 molecules were expressed in Drosophila S2 cells using the Drosophila Expression System kit (Invitrogen). Cells were co-transfected via calcium phosphate with plasmids encoding the I-A^b alpha chain or DRA*0101, the I-A^b beta chain or DRB1*0401, the BirA enzyme, and a blasticidin resistance gene at a molar ratio of 9:9:9:1. Transfected cells were selected in blasticidin containing media for 2 weeks at 28° C, passaged into serum-free media, and scaled up to 1 liter cultures in 3 liter spinner flasks. When cell densities exceeded 10^7/ml, expression was induced by the addition of 0.8 mM copper sulfate. pMHC heterodimers were purified from supernatants 4-6 days later using a His-Bind nickel affinity column (Novagen). Bound pMHC monomers were eluted according to manufacturer's instructions. Biotinylated peptide:I-A^b molecules were then separated from free biotin using a Sephacryl S-300 size exclusion column (GE Healthcare Bio-Sciences).

Tetramers were created by mixing biotinylated peptide:MHC molecules with phycoerythrin (PE) or allophycocyanin (APC) conjugated streptavidin (Prozyme) for 1 hour at room temperature. The ratio of peptide-MHC to steptavidin was determined by serial titration and Western blotting. The tetramer was then separated from excess monomer using a

Sephacryl S-300 gel filtration column. The concentration of the final product was measured at the absorbance of PE at 566 nm or APC at 650 nm.

pMHCII tetramer-based enrichment

The spleen and inguinal, axillary, brachial, cervical, mesenteric, and periaortic lymph nodes or individual thymii were harvested for each mouse analyzed. A single cell suspension was prepared in 0.2 ml of Fc block (supernatant from 2.4G2 hybridoma cells grown in serum-free media + 2% mouse serum, 2% rat serum, 0.1% sodium azide). PE- or APC-conjugated tetramer was added at a concentration of 10 nM and the cells were incubated at room temperature for 1 h, followed by a wash in 15 ml of ice-cold sorter buffer (PBS + 2% fetal bovine serum, 0.1% sodium azide). In some cases, PE- and APC-conjugated tetramers were added together at this step. The tetramer-stained cells were then suspended in a volume of 0.4 ml of sorter buffer, mixed with 0.1 ml of anti-PE antibody conjugated magnetic microbeads (Miltenyi Biotech) (and in some cases with anti-APC antibody conjugated beads), and incubated on ice for 20 minutes, followed by two washes with 10 ml of sorter buffer. The cells were then suspended in 3 ml of sorter buffer and passed over a magnetized LS column (Miltenyi Biotech). The column was washed with sorter buffer and then removed from the magnetic field. The bound cells were obtained by pushing 5 ml of sorter buffer through the column with a plunger. The resulting enriched fractions were suspended in 0.1 ml of sorter buffer, and a small volume was removed for cell counting while the rest of the sample was stained with a cocktail of fluorochrome labeled antibodies specific for B220, CD11b, CD11c, F4/80, NK1.1, CD3, CD8, CD4, or CD44. The entire stained sample was then collected on an LSR II flow cytometer (BD

Immunocytometry Systems) and analyzed using FlowJo software (TreeStar).

The percentage of tetramer-positive events was multiplied by the total number of cells in the enriched fraction to calculate the total number of tetramer positive cells in the mouse. For TCR-Vβ segment analysis, tetramer-enriched fractions from pooled or individual mouse samples were split into multiple tubes and stained as described above with the addition of Vβ-specific antibodies.

Peripheral blood analyses

Sixty ml of heparinized blood was drawn from volunteers from whom informed consent was obtained according to a protocol approved by the University of Minnesota institutional review board. Five ml of blood was used for HLA typing by the University of Minnesota Immunology/Histocompatibility Lab. Peripheral blood mononuclear cells (PBMCs) were isolated from the remaining 55 ml by Histopaque (Sigma) density gradient centrifugation according to the manufacturer's protocol. PBMCs were then analyzed for HA:DR4-specific CD4+ T cells by tetramer enrichment as described above.

Cell transfer

CD4+ T cells were purified from several naïve B6 mice using a CD4+ T cell isolation kit (Miltenyi Biotech). Half of the purified CD4+ T cells were stained with 2W1S:I-A^b tetramer and the other half with FliC:I-A^b tetramer followed by anti-PE magnetic beads as described above. Cells (~3 x 10^7) from each group that did not bind to the magnet were injected intravenously into B6 *Rag-1-/-* mice. Four days later, these mice were injected intravenously with a mixture containing 50 µg 2W1S peptide, 50

μg FliC peptide, and 5 μg LPS. Eight days later, individual recipient mice were analyzed for 2W1S:I-A^b- and FliC:I-A^b-specific CD4+ T cells by tetramer enrichment.

Peptide competition assay

The protocol was adapted from Ignatowicz et al. (87). In summary, spleen cells from *H2-DMa-/-* mice were incubated at 10^6 cells/ml in complete culture medium at 37°C for 8 hours with a limiting concentration (10 μg/ml) of $E\alpha_{52–66}$ peptide (ASFEAQGALANIAVDKA) (88) and various concentrations of the control $HA_{307-319}$ peptide or peptides of interest. The cells were then washed and stained with biotinylated anti-Ea_{52-66}:I-A^b (YAe) (88, 89) at 4°C for 30 minutes. Cells were washed and then stained with streptavidin-conjugated PE and anti-B220. Staining was measured on a LSRII (Becton Dickinson). Results were expressed as the median fluorescence intensity of the stained cells measured in arbitrary units.

Statistical methods

Standard error of the mean and p-values were determined using Prism software (GraphPad Software, Inc.). P-values were calculated using appropriate two-tailed *t* test or ANOVA analysis followed by Bonferroni post-test with a 95% confidence interval.

CHAPTER 3

Naïve CD4+ T cell frequency varies for different epitopes and predicts repertoire diversity and response magnitude

(HHC and JJM share equal contribution in this chapter)

Moon et al. Immunity. 2007 Aug;27(2):179-80.

Naive T lymphocytes become activated and proliferate when their antigen receptors (TCR) bind to cognate peptides presented on Major Histocompatibility Complex (MHC) molecules (24, 90). During infection, antigen-presenting cells display a multitude of unique foreign peptide:MHC complexes (pMHC) derived from the invading microbe. The extent to which naive T cells respond to these various pMHCs is influenced by how well antigen-presenting cells process antigenic peptides (71) and induce costimulatory ligands and cytokines (55).

It is likely that naive T cell population size also contributes to differences observed in the magnitude of the primary immune response to different antigenic peptides (91-93). However, the importance of this factor is unknown because naive T cells specific for any one pMHC are very difficult to detect due to their extremely low frequency, estimated at 100-3,000 cells per mouse (94, 95) (93, 96, 97). Because of this technical limitation, most current knowledge of naive T cell activation is based on the adoptive transfer of large numbers of monoclonal TCR transgenic T cells into histocompatible hosts (55). Although such systems have proven their use, concerns over the effects of intraclonal competition between abnormally large numbers of identical T cells have reinforced the need to study polyclonal naïve T cells directly (98, 99) (100) (77, 78). Another approach to the study of naive T cell populations relies on the use of mice in which one chain of the TCR is fixed (48, 60). The restricted diversity of the T cell repertoire in these mice results in larger than normal populations of pMHC-specific cells, thereby facilitating their study. Although the pMHC-specific T cell populations in these mice are not monoclonal, the increased sizes of these populations may still pose caveats concerning levels of competition for ligands.

In this chapter, we addressed these concerns by developing a

method using pMHCII tetramers and magnetic beads to study rare CD4+ T cell populations in unmanipulated mice. With this method, we directly measured the sizes of three distinct naive pMHCII-specific CD4+ T cell populations, and determined how this variable influences aspects of the primary immune response.

Variable CD4+ T Cell Responses to Different pMHCs

Three distinct tetramers, each consisting of four identical biotinylated peptide:I-A^b MHC molecules complexed to a fluorochrome-labeled streptavidin core, were produced to study naive polyclonal CD4+ T cell populations. The peptides used were the 2W1S variant (101) of peptide 52-68 from the I-E alpha chain (88, 102), peptide 427-441 from the FliC protein of *Salmonella typhimurium* (103), and peptide 323-339 from chicken ovalbumin (104). Each of these peptides binds to the I-A^b MHCII molecule expressed in C57BL/6 (B6) mice and is immunogenic in this strain.

These pMHCII tetramers were used in conjunction with flow cytometry in an attempt to detect naive pMHCII-specific CD4+ T cells. Spleen and lymph node cells were harvested from naive B6 mice or B6 mice injected intravenously (i.v.) 8 days earlier with the relevant peptides plus bacterial lipopolysaccharide (LPS) as an adjuvant. Peptides were used for immunization to minimize the effects of differential antigen processing between epitopes from different proteins, and an i.v. route of administration was chosen to provide a synchronous, systemic response. The cells were then stained with phycoerythrin (PE)-labeled pMHCII tetramers and antibodies specific for CD3, CD4, CD8, and a cocktail of non-T cell lineage-specific antibodies to allow for the identification of CD4+ T cells (CD3+, CD4+, non-T-lineage-, CD8- events) (Fig. 1A). Anti-CD44

antibody was also included in the staining cocktail to identify $CD44^{high}$ antigen-experienced cells (105). Although the tetramers identified expanded $CD44^{high}$ populations of different sizes in the relevant peptide-injected mice, corresponding $CD44^{low}$ populations could not be detected in naive mice (Fig. 1B). Thus, this approach lacked the sensitivity to detect naive pMHCII-specific T cells, and therefore could not be used to determine whether the differences in the sizes of the expanded populations were related to naive T cell frequency.

pMHCII Tetramer-Based Enrichment

Detection of pMHCII-specific CD4+ T cells in naïve mice was unfeasible due to the limited capacity of the flow cytometer to routinely analyze more than about 10^6 total cells, or only 1/200th of the ~2 x 10^8 nucleated cells in the lymphoid organs of a mouse, at a given time. Even if such an analysis was performed using high-speed cell sorting technology, the accumulation of low frequency background events would become prohibitive to the study of rare cell populations. The solution to these problems was to concentrate all the tetramer-binding cells from a mouse into a smaller sample containing only about 10^6 total cells, which could then be analyzed in its entirety with a high signal-to-noise ratio. This was accomplished by performing a cell enrichment step using magnetic beads coupled to antibodies specific for the PE fluorochrome component of the tetramer.

To test the efficacy of the tetramer-based enrichment, known numbers of monoclonal CD4+ T cells from SM1 TCR transgenic mice (106), which express CD90.1 and a FliC:I-A^b-specific TCR, were mixed with 2.5 x 10^8 CD90.2+ spleen and lymph node cells from a B6 mouse (Fig. 2). FliC:I-A^b tetramer staining and flow cytometry was then performed

with or without a preliminary FliC:I-A^b tetramer/anti-PE magnetic bead enrichment step. CD90.1+ events were not detected in samples lacking SM1 cells, demonstrating the absence of background tetramer staining. Without enrichment, SM1 cells were not detected until at least 1,000 were present in the mixture. In contrast, as few as 10 SM1 cells were detected using the enrichment method. Therefore, this tetramer-based enrichment method improved the limit of detection by about 100-fold, to the point where as few as 10 pMHCII-specific cells could be reliably detected in a background of 2.5 x10^8 other cells.

Remarkably, a small population of CD4+ FliC:I-A^b+ CD90.1- cells of polyclonal B6 origin was consistently detected in all of the tetramer-enriched samples (Fig. 2). This finding raised the possibility that this method could detect endogenous polyclonal pMHCII-specific naïve CD4+ T cells. Alternatively, the rare CD4+ T cells that bound the FliC:I-A^b tetramer may have done so non-specifically. These possibilities were tested by enriching spleen and lymph nodes cells from a naïve B6 mouse with a mixture of PE-labeled 2W1S:I-A^b and APC-labeled FliC:I-A^b tetramers followed by anti-PE plus anti-APC magnetic beads. As shown in Fig. 3A, this experiment resulted in the detection of two mutually exclusive CD4+ populations: one that bound FliC:I-A^b but not 2W1S:I-A^b, and a larger one that bound 2W1S:I-A^b but not FliC:I-A^b. The absence of CD4+ T cells that bound both tetramers ruled out the possibility that non-specific binding was responsible for the enrichment of these distinct populations of cells.

Several other pieces of evidence indicated that tetramer-binding T cells detected by the enrichment method were truly pMHCII-specific cells. First, the 2W1S:I-A^b+ cells detected in a 2W1S:I-A^b tetramer-enriched sample from a naïve B6 mouse had the $CD44^{low}$ phenotype of naïve T cells

(Fig. 3B). Second, few if any of these cells expressed CD8 (Fig. 3B), which marks pMHCI-specific T cells. Third, few if any 2W1S:I-A^b+ T cells were detected in the CD4+ or CD8+ T cells of a 2W1S:I-A^b tetramer-enriched sample of spleen and lymph nodes cells from an $OVA_{257-264}$:K^b specific TCR transgenic OT-I mouse (32) (Fig. 3C), or an $OVA_{323-339}$:I-A^b TCR transgenic OT-II mouse (107) (Fig. 3D). The few $CD44^{low}$, CD4+, 2W1S:I-A^b+ cells detected in the OT-II sample likely expressed a 2W1S:I-A^b-specific TCR produced by rearrangement of an endogenous TCR-Vα chain, which can occur in TCR transgenic mice expressing RAG proteins (75). This contention was supported by the finding that no CD4+, 2W1S:I-A^b+ cells were detected among spleen and lymph node cells from a RAG-deficient OT-II TCR transgenic mouse, or in two other TCR transgenic RAG-deficient lines containing monoclonal T cells specific for other pMHCII (Fig. 3E). Together, these results indicated that the tetramer-based enrichment method was sensitive enough to detect rare naïve CD4+ T cells specific for individual pMHCII.

If the cells detected by tetramer-based enrichment were truly naïve pMHCII-specific CD4+ T cells, then they should show signs of activation when exposed to the relevant peptide. As shown in Fig. 4A, about 50% of the 2W1S:I-A^b+ CD4+ T cells in B6 mice injected i.v. 48 hours earlier with 2W1S peptide plus LPS expressed high levels of CD44 and/or had undergone blastogenesis compared to about 5% of the cells in mice that were injected with LPS alone. This result could not be explained by preferential expansion of a small number of cells in the peptide-injected mice because the numbers of 2W1S:I-A^b+ CD4+ T cells present in the 2 groups of mice were similar at this early time (Fig. 5C). In addition, 2W1S:I-A^b+ T cells in a dye-labeled B6 CD4+ T cell population transferred into B6 hosts did not show signs of cell division 48 hours after injection of

2W1S peptide plus LPS (data not shown). These results showed that peptide responsive naïve CD4+ T cells were detected by the tetramer enrichment method. The efficiency of tetramer-based enrichment was measured by assaying its capacity to deplete a target population from a polyclonal sample. Purified CD4+ T cells (~4 x10^7) from naïve B6 mice were stained with either 2W1S:I-A^b or FliC:I-A^b tetramer. The stained samples were then passed over a magnetized column, and the ~4 x 10^7 cells that did not bind were transferred into lymphocyte-deficient *Rag-1-/-* mice, which were then injected intravenously with a mixture of FliC and 2W1S peptides plus LPS. Eight days later, the number of 2W1S:I-A^b+ or FliC:I-A^b+ cells in the recipient mice was measured by tetramer-based enrichment. As shown in Figure 4B, *Rag-1-/-* mice reconstituted with 2W1S:I-A^b-depleted cells contained a population of $CD44^{high}$ FliC:I-A^b+ cells but not 2W1S:I-A^b+ cells, whereas *Rag-1-/-* mice reconstituted with FliC:I-A^b depleted cells contained a large population of $CD44^{high}$ 2W1S:I-Ab+ cells but very few FliC:I-A^b+ cells following immunization. These results demonstrated that most, if not all of the relevant pMHCII-specific CD4+ T cells in a naïve mouse were captured by the magnetic column.

Naive CD4+ T Cell Population Sizes

The specificity and efficiency of tetramer-based enrichment allowed for the accurate enumeration of naive CD4+ T cells specific for 2W1S:I-A^b, FliC:I-A^b, or OVA:I-A^b. Individual naïve B6 mice contained on average 190 2W1S:I-Ab-specific, 20 FliC:I-A^b-specific, and 16 OVA:I-A^b-specific CD4+ T cells in their spleen and lymph nodes (Fig. 5A, B). Each of these values was significantly greater (Student's T-test, two-tailed, $P < 0.001$) than the values for CD8+ cells in the same samples or irrelevant TCR transgenic T cells stained with the same tetramers (Fig. 5B). The ~5 CD8+ cells per

mouse that were detected with each pMHCII tetramer may have been rare CD8+ pMHCII-specific T cells similar to those discovered in *CD4-/-* mice (108, 109). The number of 2W1S:I-A^b-specific CD4+ T cells was significantly greater than the numbers of FliC:I-A^b- or OVA:I-A^b-specific T cells ($P < 0.001$), which were not significantly different from each other ($P = 0.48$). Therefore, while the sizes of individual naïve CD4+ T cell populations were highly consistent amongst individual mice, these populations varied in size depending on their pMHCII specificity.

pMHCII-Specific CD4+ T Cell Population Sizes Following Immunization

The naive 2W1S:I-A^b-, FliC:I-A^b-, or OVA:I-A^b-specific populations were roughly proportional in size to the corresponding expanded populations observed in peptide injected mice (Fig. 1B). This relationship was explored in more detail using the enrichment method over a three-week period following i.v. injection with the relevant peptides plus LPS (Fig. 5C). The 2W1S:I-Ab-specific population increased about 300-fold to a peak of ~80,000 cells by day 6. The FliC:I-A^b- and OVA:I-A^b-specific populations also increased about 300-fold to 5,000 and 3,000 cells during the same period. Since all three populations expanded at similar rates over the first 6 days after peptide injection, the larger number of 2W1S:I-Ab-specific cells present at these times was likely related to the corresponding larger naïve population. After day 6, the relationship between pre- and post-immunization frequency was less clear because the 2W1S:I-A^b-specific population was contracting while the FliC:I-A^b- and OVA:I-A^b specific populations continued to increase.

The correspondence between naïve population size and response magnitude was further confirmed in a peptide dose response experiment.

As shown in Fig. 5D, the number of 2W1S:I-A^b-specific T cells was significantly greater than the number of FliC:I-A^b- and OVA:I-A^b-specific T cells 4 days after peptide/LPS injection at all doses of peptide tested ($P < 0.05$). Thus, the greater magnitude of the 2W1S-specific T cell response is likely due to higher precursor frequency rather than more efficient peptide presentation.

TCR Variable Segment Diversity

Analysis of TCR variable gene usage as a measure of clonal diversity provided additional evidence for variation in naïve population sizes. The naive 2W1S:I-A^b-specific population consistently displayed a V segment usage pattern that was distinct from that of the total CD4+ T cell population (Fig. 6A and B). Cells expressing Vβ4, Vβ5, or Vβ11 were overrepresented in the 2W1S:I-Ab-specific population, whereas cells expressing Vβ6, Vβ8, Vβ12, Vβ14, and Vα2 were underrepresented. This distinct V segment usage pattern was preserved in the expanded population of 2W1S:I-A^b-specific cells 4 days after intravenous injection with 2W1S peptide plus LPS (Fig. 6A and B). The similarity between pre- and post-immunization V segment usage indicated that most of the cells in the naïve 2W1S:I-A^b-specific repertoire proliferated during the early stages of the primary immune response.

These results suggested that V segment usage by an expanded T cell population is reflective of the naïve starting population. Therefore, V segment usage in the FliC:I-A^b- and OVA:I-A^b-specific naïve populations, which were too small to study directly with multiple anti-V segment antibodies, could be estimated from their corresponding expanded populations. By pooling tetramer-enriched cells from mice 8 days after peptide injection, it was possible to assess usage of all Vβ segments for

which antibodies are available. The expanded population of 2W1S:I-A^b-specific T cells was very diverse (Fig. 6C), containing cells expressing each of the 14 Vβ segments tested, but with overrepresentation of Vβ4, 5, and 11 compared to the total population of CD4+ T cells. In contrast, the smaller populations of FliC:I-A^b- and OVA:I-A^b-specific cells were much less diverse. The FliC:I-A^b-specific population was dominated by cells expressing Vβ8 or Vβ12 whereas the OVA:I-A^b-specific population was comprised primarily of cells expressing Vβ4, Vβ5, or Vβ8. Since each clone expresses a single Vβ segment, the presence of fewer Vβ segments in the smaller populations is consistent with the possibility that they are comprised of fewer clones than the larger 2W1S:I-A^b-specific population.

Analysis of cells from individual mice provided additional evidence for small FliC:I-A^b- and OVA:I-A^b-specific populations (Fig. 6D). Vβ usage among these populations was much more variable than in the case of 2W1S:I-A^b-specific populations. In some individual mice, the FliC:I-A^b and OVA:I-A^b-specific populations were dominated by cells expressing only one of the preferred Vβ segments, whereas in other mice the population contained at least 4 different Vβ segments. Collectively, the limited diversity of the FliC:I-A^b- and OVA:I-A^b-specific populations and their greater susceptibility to individual variation reinforced the finding that their corresponding naïve precursor frequencies are smaller than that of the 2W1S:I-A^b-specific population.

Discussion

Since Klinman's pioneering studies on the frequency of naïve B cells (110), numerous efforts have been made to address this issue with respect to epitope-specific naïve T cells. Collectively, past work produced estimates ranging from 100 to 3,000 cells depending on the epitope in

question (93-97). Most of the methods used to arrive at these values relied on indirect means of detection. For example, one approach involved titration of TCR transgenic T cells into normal mice, which were then exposed to the relevant antigen (94, 95, 97). The number of transferred cells that produced an antigen expanded population equal to that produced from the host was assumed to reflect the number of host precursors. In addition, some of these studies involved sampling only a small fraction of the total lymphoid cells in a mouse, thereby necessitating large extrapolation factors to calculate total cell numbers. Finally, all of the early studies produced estimates for only one epitope-specific population, precluding a definitive comparison of different population sizes.

Many of these limitations were overcome in the current study. Identification of epitope-specific CD4+ T cells was based directly on pMHCII binding. A novel enrichment step allowed comprehensive sampling of the entire secondary lymphoid compartment of a mouse, thereby avoiding the need for large extrapolation factors in the calculation of T cell frequency. The use of exclusion gating and relevant negative controls allowed detection of as few as 5 cells per mouse. For these reasons, the values obtained here for naive CD4+ T cell population sizes are likely the most accurate obtained to date, with the caveat that they may be slight underestimates due to cell loss during manipulations and the fact that blood and mucosal-lymphoid tissues were not sampled.

The values reported here for the number of epitope-specific CD4+ T cells allows for estimation of the number of epitopes that could be recognized by the naïve repertoire. Assuming that each pMHCII-specific CD4+ T cell population consists of about 100 cells and that there are about 3×10^7 naive CD4+ T cells in a mouse, it follows that at least 3×10^5 unique pMHCII specificities exist within the naive repertoire. However,

this is likely a minimum value because individual T cells have been shown to recognize more than one pMHC (111, 112).

Although the naïve populations studied in this report clearly contained multiple clones as evidenced by diverse Vβ usage, the precise number of clones in each is not clear. Extensive TCR sequence analysis by Casrouge et al. showed that individual mice contain about 2 x 10^6 distinct naïve αβ TCR clones of 10 cells each in the spleen (113). Our findings indicated that the naive populations of FliC:I-A^b- and OVA:I-A^b-specific T cells numbered only about 20 per mouse, and that in some individual mice these populations contained cells expressing one of at least 4 different Vβ segments (Fig. 6D). Therefore, because each T cell expresses only one Vβ segment, these populations must consist of at least 4 clones each. Indeed, it is possible that each cell in each population was a unique clone in which case our results would be more in line with the recent finding that 50-550 distinct CD8+ T cell clones recognize each epitope in individual mice (114).

Our results indicate that polyclonal CD4+ T cell populations expand in proportion to the frequency of their naïve progenitors, at least during the early phase of the primary immune response. Thus, at least for certain peptides, variations in naïve CD4+ T cells population size may account for the observation that the number of T cells generated at the peak of the primary immune response to infection varies for different pMHCII (91, 92, 115).

Notably, not all of the 2W1S:I-A^b tetramer-binding cells in naïve mice showed signs of activation 48 hours after peptide immunization. Our findings that pMHCII tetramer-binding cells were not detected in CD8+ populations or in mice containing irrelevant monoclonal T cells provides strong evidence that tetramer binding was indeed TCR-specific. Thus, the

tetramer-binding cells were unlikely to be background events. On the contrary, the non-responsive tetramer-binding cells may have simply not encountered a stimulatory antigen-presenting cell in the 48 hour time frame. This is supported by our finding that the TCR diversity of the naive 2W1S:I-A^b-specific T cell population was preserved after four days of antigen-induced proliferation, implying that a high percentage of this naive repertoire eventually participated in the response. This conclusion is in agreement with a previous study on another pMHCII-specific CD4+ T cell population (60). Alternatively, the non-responders may have possessed TCRs with too low an affinity to become activated at the peptide dose administered. Finally, these cells may have been recent thymic emigrants that have been reported to be inherently hyporesponsive to antigenic stimulation (116).

Naive CD8+ T cell populations that vary in size have been reported to peak at the same time following immunization (91, 92). In contrast, we found that a relatively large naive CD4+ T cell population peaked earlier than two smaller populations, as predicted by earlier experiments with adoptively transferred TCR transgenic T cells (78). Because the large and small populations increased with the same initial kinetics, it is possible that the large population became numerous enough to compete for limiting pMHCII, resulting in an earlier cessation of the response. This is plausible because unlike CD8+ T cells (117-119), CD4+ T cells only continue to proliferate in the presence of pMHC (120). Differences in pMHCII persistence at later times after immunization may explain why the FliC:I-A^b- and OVA:I-A^b-specific populations eventually diverged.

Our findings indicate that large naïve populations contain more distinct clones than small populations, rather than more copies of each clone. Large naïve populations may exist for those foreign pMHCII that

have properties, for example charge and hydrophobicity, which are conducive to recognition by many structurally distinct TCRs. In contrast, the properties of other foreign pMHCII, for example similarity to self-pMHCII, may be conducive to recognition by only a small number of TCRs due to strong thymic negative selection. Our results agree with other studies suggesting that such populations can be small enough that it becomes unlikely that the random process of *Tcr* gene rearrangement will produce identical sets of clones in individual mice (121). Immune responses that depend on very small naïve populations may be inherently variable and at risk for extinction under conditions where total lymphocyte numbers are reduced, such as aging, chemotherapy, and HIV infection (122).

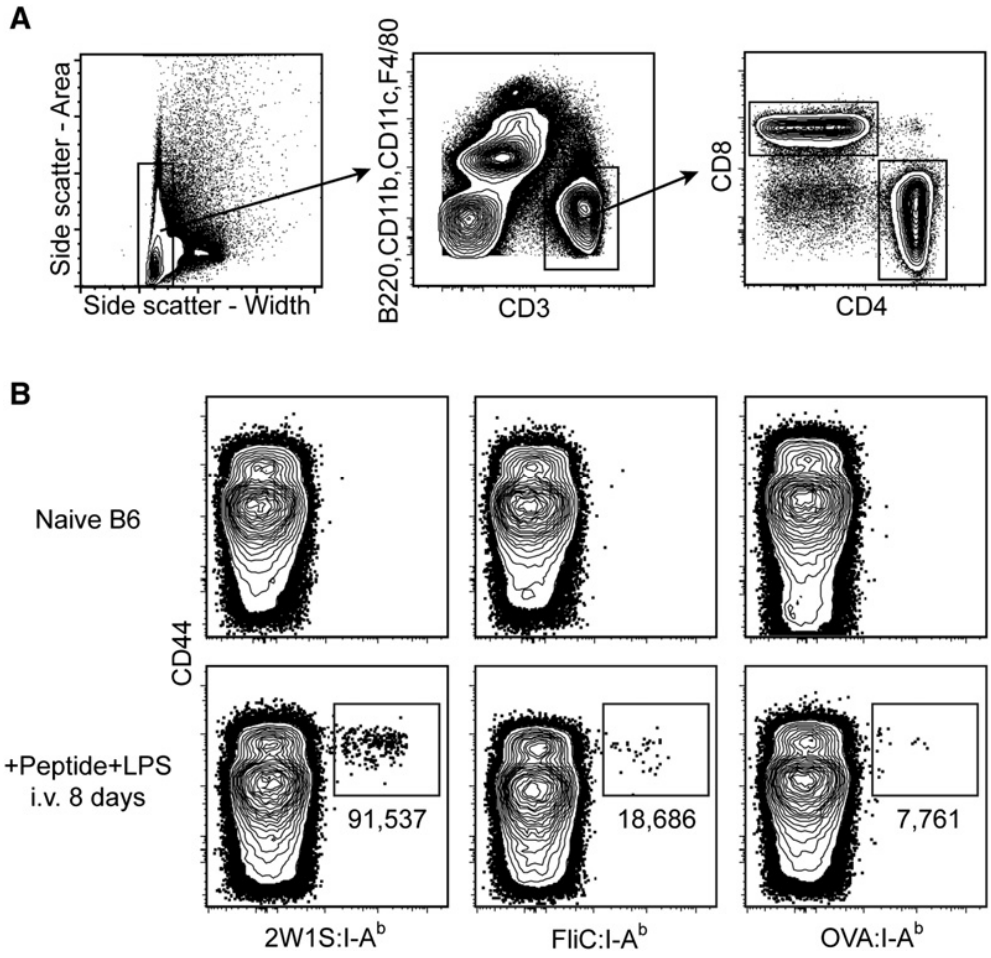

Figure 1: Primary immune responses of naive CD4+ T cells vary with respect to pMHC specificity. A, Flow cytometry gates used in all figures to identify T cells from total spleen and lymph node cells: side scatter-widthlow (left plot); CD3+, non-T cell lineage- (middle plot); and either CD4+ or CD8+ (right plot). **B,** Where indicated, B6 mice were injected i.v. with 50 μg of the indicated peptide plus 5 μg LPS. Eight days later, spleen and lymph node cells were harvested and stained with the indicated tetramer. Representative contour plots of CD44 versus the indicated tetramers are shown for non-T cell lineage-, CD3+, CD4+ events gated from 106 total collected events. The total number of cells for each individual mouse shown is indicated below the relevant gate. Mean values ± S.D. were 2W1S: 115,000 ± 40,000; FliC: 23,000 ± 20,000; OVA: 7,000 ± 3,000 (n=4 per group).

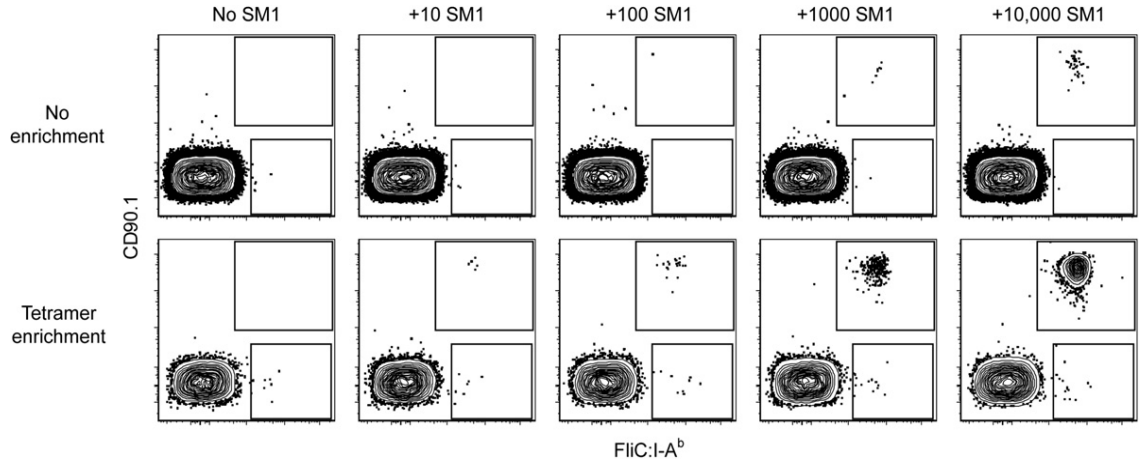

Figure 2: Tetramer-based enrichment increases the sensitivity of detection of epitope-specific T cell populations. Representative contour plots of CD90.1 versus FliC:I-A^b for CD4+ gated events from mixtures of 2.5 x 10^8 B6 spleen and lymph node cells and the indicated numbers of SM1 TCR transgenic T cells analyzed directly (top row) or after tetramer-based enrichment (bottom row). SM1 cells are shown in the upper gate and polyclonal FliC:I-Ab-specific CD4+ T cells in the lower gate. Data are representative of two independent experiments.

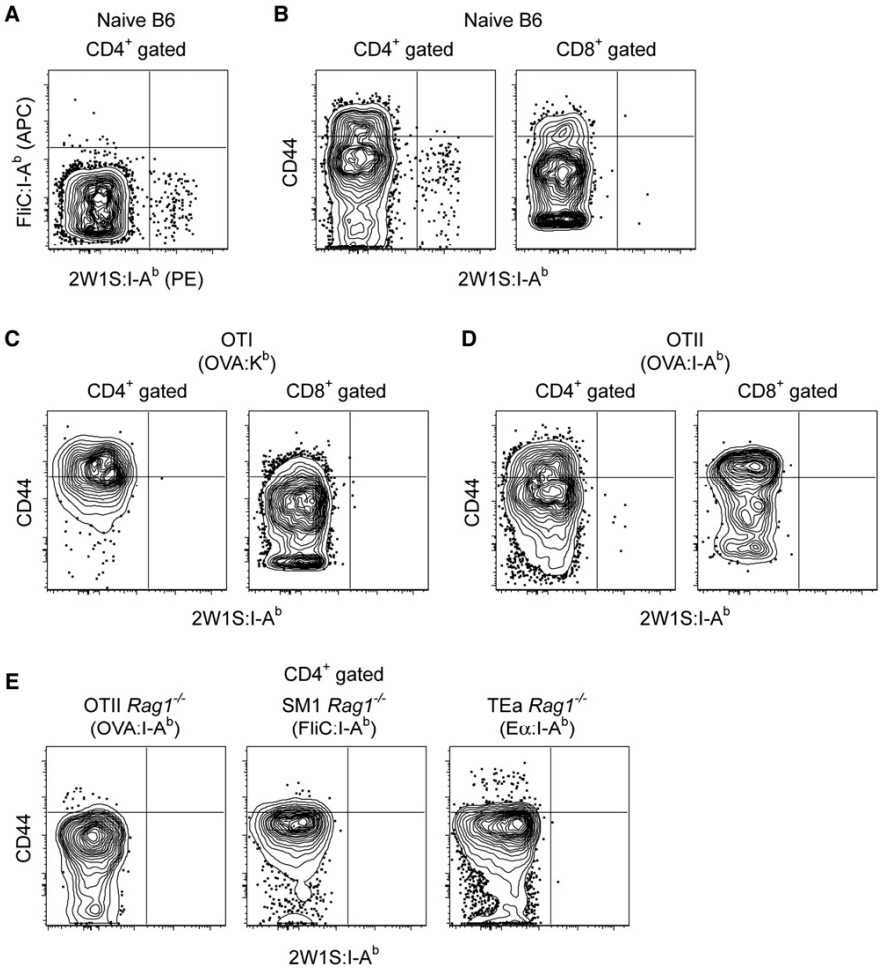

Figure 3: Naïve pMHCII-specific CD4+ T cells can be detected using tetramer based enrichment. A, Representative contour plot of FliC:I-A^b tetramer (APC) versus 2W1S:I-A^b tetramer (PE) for non-T cell lineage-, CD3+, CD4+ events in a spleen and lymph node cell population from a naive B6 mouse after enrichment with FliC:I-A^b and 2W1S:I-A^b tetramers. **B,** Representative contour plots of CD44 versus 2W1S:I-A^b for CD4+ or CD8+ gated events following 2W1S:I-Ab tetramer enrichment of total spleen and lymph node cells from a naive B6 mouse, or **C,** an OT-I *Rag-1-/-*, or **D,** an OT-II *Rag-1+/+* TCR transgenic mouse. **E,** Representative contour plots of CD44 versus 2W1S:I-A^b for CD4+ gated events following 2W1S:I-A^b tetramer enrichment of total spleen and lymph node cells from OT-II *Rag-1-/-*, SM1 *Rag-1-/-*, and TEa *Rag-1-/-* TCR transgenic mice. Data are representative of at least 3 independent experiments.

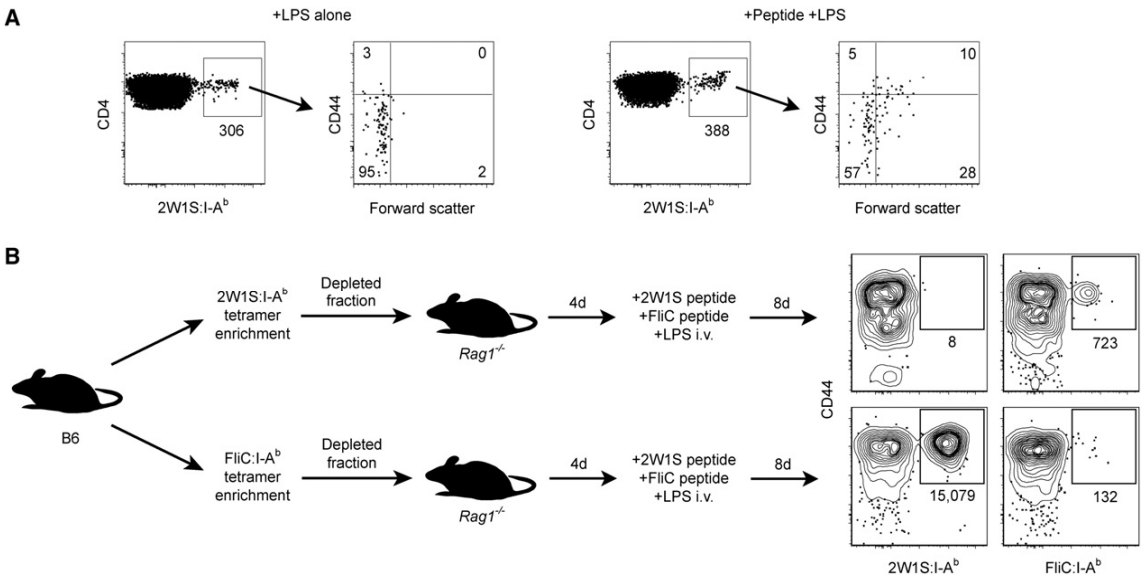

Figure 4: Tetramer-binding T cells are responsive to their relevant peptide. A, 2W1S:I-A^b enrichment was performed on total spleen and lymph node cells from B6 mice injected i.v. 48 hours earlier with 5 µg LPS (left panels), or 5 µg LPS plus 250 µg 2W1S peptide (right panels). CD4+, 2W1S:I-A^b+ events were then analyzed for CD44 expression and blastogenesis (forward scatter). Numbers indicate percentages of events in each quadrant. Data are representative of at least 3 independent experiments. **B,** Contour plots of CD44 versus tetramer for 2W1S:I-A^b or FliC:I-A^b enriched spleen and lymph node cells from B6 *Rag-1-/-* hosts that received either 2W1S:I-A^b or FliC:I-A^b tetramer-depleted cells from naïve B6 mice, and were then injected i.v. with a mixture of 50 µg 2W1S peptide, 50 µg FliC peptide, and 5 µg LPS 8 days before analysis. The total number of tetramer+ cells for each population is shown below the relevant gate. Data shown are representative of three independent experiments.

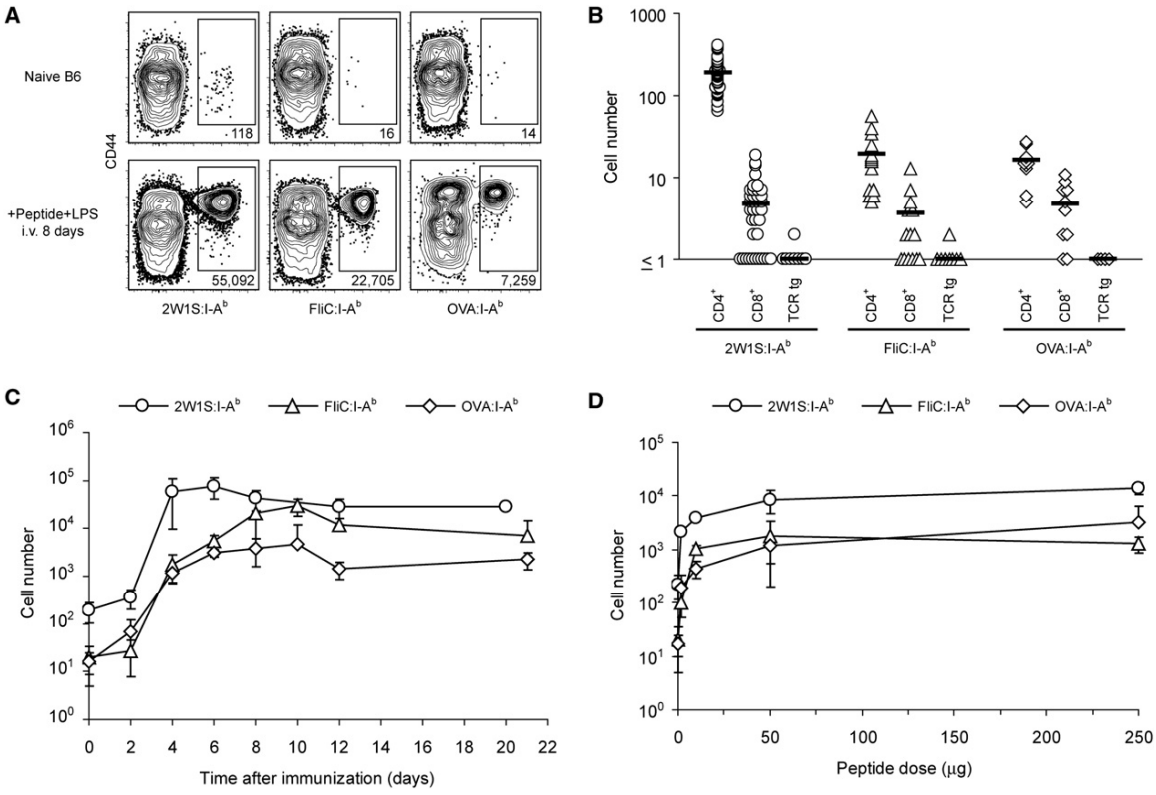

Figure 5: Naive CD4+ T cell populations vary in size. A, Representative contour plots of CD44 versus tetramer for CD4+ events from total spleen and lymph node cells from naive B6 mice (top row) or B6 mice injected i.v. with 50 µg of the indicated peptide plus 5 µg LPS (bottom row) following enrichment with the indicated tetramers. **B,** Total numbers of tetramer+, CD4+ or CD8+ cells following tetramer enrichment of total spleen and lymph node cells from a naive B6 mouse or tetramer+, CD4+ cells from OT-II *Rag-1-/-*, TEa *Rag-1-/-*, or SM1 *Rag-1-/-* TCR transgenic mice. Symbols represent individual mice; horizontal bars indicate mean values. **C,** Mean total number (±S.D., n=2-8) of 2W1S:I-A^b+ (circles), FliC:I-A^b+ (triangles), or OVA:I-A^b+ (diamonds) cells in B6 mice over time following i.v. injection with 50 µg of the relevant peptide plus 5 µg LPS. **D,** Mean total number (±S.D., n=3) of 2W1S:I-A^b+ (circles), FliC:I-A^b+ (triangles), or OVA:I-A^b+ (diamonds) cells in B6 mice 4 days following i.v. injection with 5 µg LPS plus the indicated amount of relevant peptide.

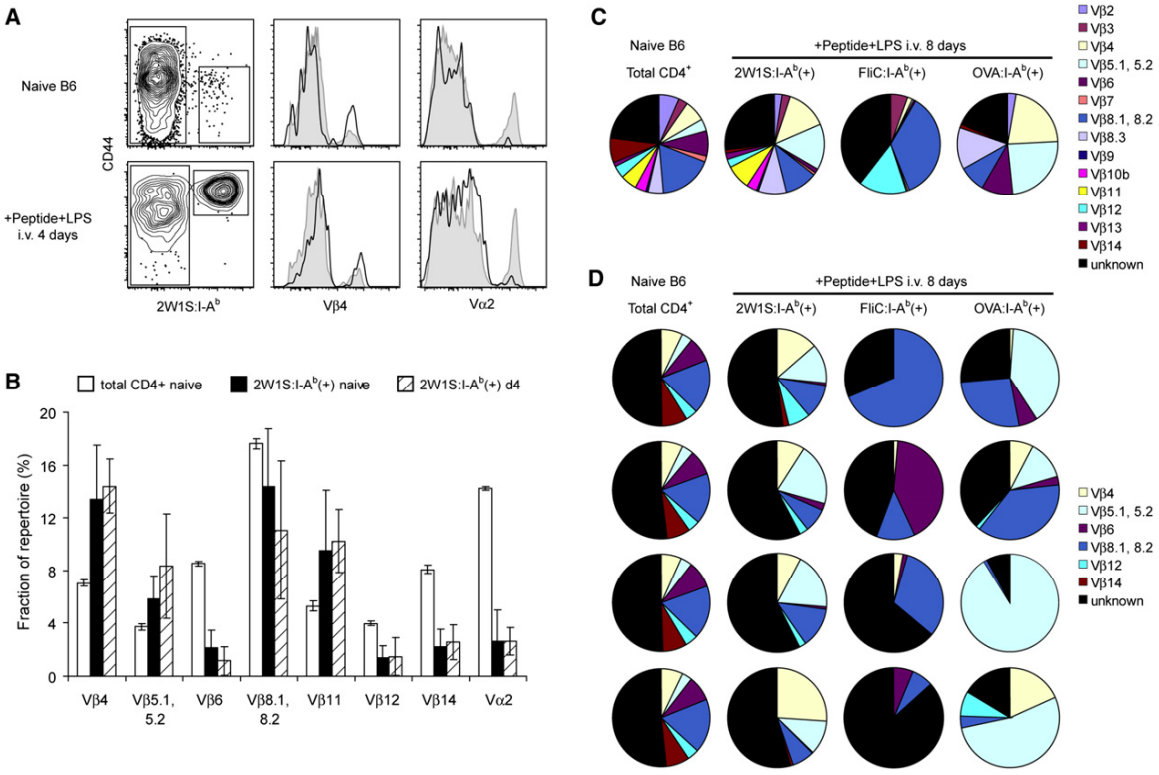

Figure 6: Naive CD4+ T cell population diversity is related to population size. A, Total lymph node and spleen cells from naive B6 mice (top) or B6 mice injected i.v. with 50 µg 2W1S peptide plus 5 µg LPS 4 days earlier (bottom) were stained with antibodies to TCR Vβ4 and Vα2. 2W1S:I-A^b- and 2W1S:I-A^b+ gated events are represented in histograms by shaded profiles and solid lines, respectively. **B,** TCR Vβ and Vα gene segment usage in total CD4+ T cells from naive mice (unfilled bars), or 2W1S:I-A^b+ CD4+ T cells from naive mice (filled bars) or mice injected i.v. with 50 µg 2W1S peptide plus 5 µg LPS 4 days earlier (hatched bars). Data are mean values + S.D. from 4-8 mice per group. **C,** Usage profile for TCR Vβ gene segments in total CD4+ T cells from naïve B6 mice or tetramer+ CD4+ T cells from B6 mice injected i.v. with 50 µg of the indicated peptide plus 5 µg LPS 8 days earlier. Data are values from pooled samples taken from 4-10 mice per group, or **D,** samples taken from 4 individual mice per group.

CHAPTER 4

Positive selection optimizes the number and function of MHCII-restricted CD4+ T cell clones in the naïve polyclonal repertoire

Chu et al. Proc Natl Acad Sci U S A. 2009 Jul 7;106(27):11241-5.

Each T cell expresses a unique T cell receptor (TCR) capable of binding to a short peptide embedded in a major Histocompatibility complex (MHC) molecule on the surface of host cells (24, 123). The repertoire of matureTcells found in a given individual contains clones capable of responding to foreign peptides bound to the type of MHC encountered in the thymus of that individual. This property of T cell antigen recognition is known as MHC restriction (16). The T cell repertoire is also self-tolerant, due in large part to intrathymic negative selection via apoptosis of clones that express TCRs with a high affinity for self peptides bound to self MHC molecules (124).

T cell clones with these features are thought to be selected from a large pool of immature cells based on the affinity of their TCRs for the MHC molecules encountered in the thymus (30). Evidence supporting this hypothesis comes from bone marrow chimera experiments in which mice homozygous for MHC allele A (MHC^A) are irradiated and transplanted with F_1 bone marrow cells coexpressing MHC^A and a different allele, MHC^B. Immunization of these chimeras with a foreign antigen produces T cell responses specific for immunogen-derived foreign-peptide:MHC^A that are at least 50 times larger than those specific for immunogen-derived foreign-peptide:MHC^B, despite the fact that antigen-presenting cells in these mice express both MHC^A and MHC^B (31, 125).

This restricted recognition of foreign peptide:MHC^A by mature T cells has been explained by the phenomenon of positive selection (30). It has been shown that low affinity TCR binding to self-peptide:MHC^A on radio-resistant thymic epithelial cells is required for a T cell clone to complete development in the MHC^A thymus (32, 33). Low affinity for a self-peptide:MHC^A is thought to predispose a T cell clone to high affinity recognition of a foreign-peptide:MHC^A.

Analyses of transgenic mice expressing a single TCR have also yielded evidence for positive selection. For almost all of the TCR transgenic lines studied to date, mature T cells only develop in the presence of the form of MHC expressed by the strain from which the original T cell clone was derived (30, 126). Although only a relatively small number of different TCR transgenic lines have been tested (30), results from these lines indicate that foreign-peptide:MHC^A-specific T cells survive selection in MHC^A but not MHC^B hosts.

The aforementioned studies relied on monoclonal T cells or post-immune polyclonal T cells. Thus, the question still remains: how does positive selection shape the polyclonal preimmune repertoire in normal individuals? Assessment of the normal situation would require analysis of a foreign-peptide:MHC^A-specific T cell population in the preimmune polyclonal repertoires of normal individuals that do or do not express MHCA. In this chapter, we performed this experiment in mice and humans using the sensitive method of peptide:MHC tetramer/magnetic bead-based enrichment.

Detection of Naive Foreign-Peptide:MHC^A-Binding T Cells in Mice Expressing MHC^B

Positive selection had not been studied in the pre-immune polyclonal T cell repertoire because individual foreign-peptide:MHC-specific populations are extremely small. Recently, however, we (127) and then others (128-130) overcame this problem using peptide:MHC tetramers and magnetic bead-based enrichment (79) to identify naive foreign-peptide:MHC-specific T cells in mice. This technique has the capacity to identify most if not all of the relevant T cells in a mouse with a limit of detection of about 5 cells per mouse (127).

Tetramer enrichment was initially used to study the T cell repertoires of inbred mouse strains. Two peptide:murine MHCII tetramers were used for this purpose. Both tetramers contained the I-A^b MHCII molecule expressed by the C57BL/6 (B6) strain. One contained a peptide called 2W1S, which is a variant of an I-A^b binding peptide from the alpha chain of the murine I-E^d MHCII molecule (101). The other tetramer contained peptide 427–441 from the FliC protein of *Salmonella typhimurium* (103) Both peptides are immunogenic in B6 mice (101, 103, 127).

These tetramers were used with magnetic enrichment to enumerate peptide:I-A^b-specific naive T cells in mouse strains expressing I-A^b (B6) or other MHCII molecules (BALB/c and NOD). As expected based on past work (127), each naive B6 mouse contained small populations of CD4+ (Fig. 7A) $CD44^{low}$ 2W1S:I-A^b+ and FliC:I-A^b+ T cells in the spleen and lymph nodes (Fig. 7B). Remarkably, 2W1S:I-A^b+ and FliC:I-A^b+ CD4+ T cells were also detected in the spleen and lymph nodes of BALB/c and NOD mice (Fig. 7B), which express I-A^d and I-E^d, or I-A^{g7} molecules. The T cells in all strains were detected via specific binding of the tetramers to the relevant TCRs as evidenced by the finding that the 2 tetramers detected mutually exclusive populations (Fig. 7B). In addition, each tetramer stained very few CD8+ T cells [~5 per mouse (127)], or CD4+ T cells from TCR transgenic lines (107, 131) that could only recognize ovalbumin peptide:MHCII ligands (Fig. 7C). B6 and BALB/cmice contained about 170 2W1S:I-A^b+ and 30 FliC:I-A^b+ naive CD4+ T cells in the spleen and lymph nodes (Fig. 7D). C.B10-*H2b* and B6.C-*H2d* mice had 339 ±14 (n = 3) and 84 ± 12 (n = 3) 2W1S:I-A^b+ CD4+ T cells, respectively. In contrast, NOD mice contained about 600 2W1S:I-A^b+ and 160 FliC:I-A^b+ CD4+ T cells (Fig. 7D). FVB (H-2q) mice contained twice as many 2W1S:I-A^b+ naive CD4+ T cells (586 ± 113, n = 5) as B6 mice.

A similar situation was observed in the thymus. Tetramer enrichment was performed on all of the thymocytes from individual 6–8 week old mice. Mutually exclusive 2W1S:I-A^b- and FliC:I-A^b- binding cells were detected in the CD4SP but not CD8SP thymocyte populations (Fig. 7A) in B6, BALB/c, and NOD mice (Fig. 7B). The average sizes of the 2W1S:I-A^b+ CD4SP populations in B6, BALB/c, and NOD mice were 180, 130, and 245 cells per mouse, respectively, whereas the FliC:I-A^b+ CD4SP populations in both B6 and BALB/c strains were 15 cells per mouse and 45 cells per NOD mouse (Fig. 7D). Therefore, foreign-peptide:I-A^b-binding CD4+ T cells were generated in the thymuses and exported to the periphery in mice that expressed I-A^d and I-E^d at the same frequency as in mice that expressed I-A^b molecules, and at an even higher frequency in mice that expressed I-A^{g7}.

Foreign Peptide:I-A^b-Specific T Cell Populations in B6 and BALB/c Mice Have Different Compositions

Although the foreign-peptide:I-A^b-binding CD4+ populations in B6 and BALB/c mice were numerically similar, the fine specificity of their constituent clones could have been different. This was a likely possibility because the population in B6 but not BALB/c mice was subjected to negative selection by self-peptide:I-A^b complexes. Radiation bone marrow chimeras were used to address this point. (B6 x BALB/c) F_1 bone marrow cells were injected into lethally irradiated BALB/c (I-A^d/I-E^d) or B6 (I-A^b) hosts to produce F_1 > BALB/c or F_1 > B6 chimeras. Because negative selection is caused mainly by radio-sensitive bone marrow-derived cells (132) and positive selection by the radio-resistant thymic epithelium (133) (Fig. 8A), the T cell repertoires in these mice would be expected to be devoid of clones with high affinity for self peptides bound to I-A^b, I-A^d, and

I-E^d molecules, and positively selected for clones with low affinity for self peptides bound to either I-A^b or I-A^d and I-E^d molecules.

F_1 > B6 chimeras had significantly more naive 2W1S:I-A^b+ or FliC:I-A^b+ CD4+ T cells in the spleen and lymph nodes than F_1 > BALB/c chimeras (225 versus 48, and 47 versus 18, respectively) (Fig. 8B). Similarly, the number of 2W1S:I-A^b+ CD4SP thymocytes in F_1 > B6 chimeras (139 ± 39, *n* = 4) was significantly greater ($P < 0.001$) than the number in F_1 > BALB/c chimeras (15 ± 3, *n* = 4). Therefore, when negative selection was induced by self-peptides bound to I-A^b, I-A^d, and I-E^d molecules, naive foreign-peptide:I-A^b-specific CD4+ T cell populations were larger when positively selected in thymuses expressing I-A^b than in thymuses expressing I-A^d/I-E^d molecules. This finding indicated that many clones in the foreign-peptide:I-A^b-specific populations in intact BALB/c mice were also specific for self-peptide:I-A^b complexes. The presence of these ‘‘alloreactive’’ clones indicated that the 2W1S:I-A^b+ and FliC:I-A^b+ CD4+ T cell populations in BALB/c mice had a different clonal composition than the comparable populations in B6 mice.

Foreign-Peptide:I-A^b-Specific T Cell Populations in BALB/c Mice Are Less Functional Than Those in B6 Mice

The differences in fine specificity raised the possibility that the T cell populations in B6 and BALB/c mice might respond differently to immunization. The activation of 2W1S:I-A^b-binding CD4+ T cells in B6 and BALB/c mice was assessed 5 days after i.v. injection of 2W1S peptide plus the adjuvant lipopolysaccharide (LPS) to test this possibility. As shown in Fig. 9A, this injection induced the naive 2W1S:I-A^b+ population in B6 but not BALB/c mice to undergo robust clonal expansion and conversion to the $CD44^{high}$ phenotype. However, this was probably not a true test of the

function of the 2W1S:I-A^b-binding T cells in BALB/c mice because I-A^d or I-E^d molecules would present the 2W1S peptide in this case.

To circumvent this problem, activation was measured 5 days after i.v. injection of F_1 spleen cells that were pulsed in vitro with 2W1S peptide. In this case, the 2W1S:I-A^b-binding T cells in both strains would be exposed to 2W1S:I-A^b complexes on the F_1 antigen-presenting cells. As shown in Fig. 9B, injection of 2W1S-pulsed F_1 spleen cells into B6 mice stimulated the naive 2W1S:I-A^b+ population to undergo marked clonal expansion and conversion to the $CD44^{high}$ phenotype, whereas injection of unpulsed F_1 spleen cells did not. 2W1S-pulsed but not unpulsed F1 spleen cells also stimulated the naive 2W1S:I-A^b+ population in BALB/c mice to convert to the $CD44^{high}$ phenotype and undergo some expansion (Fig. 9B and C). The expansion was much less than that observed in B6 mice (Fig. 9C, $P < 0.01$), suggesting that the naive 2W1S:I-A^b+ population in BALB/c mice was less functional than that in B6 mice. Again, however, it is possible that this experiment was not a fair test of the functionality of the BALB/c population. The F_1 spleen cells were certainly rejected by both B6 and BALB/c recipients. This process could have released the 2W1S peptide from the F_1 cells such that it could be bound by I-A^b molecules on recipient antigen-presenting cells and re-presented to the naive 2W1S:I-A^b+ T cells. Because this type of re-presentation may not occur in BALB/c mice, the naive 2W1S:I-A^b+ population in BALB/c mice would be at a disadvantage.

Radiation bone marrow chimeras were again useful for addressing this issue. F_1 > B6 and F_1 > BALB/c chimeras both contained F_1 antigen-presenting cells capable of producing peptide:I-A^b complexes, and contained T cell repertoires that were tolerant of self-peptide:I-A^b complexes. The only difference was that one repertoire was positively

selected on I-A^b and the other on I-A^d/I-E^d (Fig. 8A). The capacity of peptide:I-A^b-specific T cells in these mice to respond to an antigen was tested by injection of 50 µg of 2W1S peptide plus LPS. The population of ~200 2W1S:I-A^b+ T cells in naive F1 > B6 chimeras increased 120-fold to 24,000 cells 6 days after injection, whereas the initial population of 40 cells in naive F_1 > BALB/c chimeras increased only 16-fold to 640 cells (Fig. 10A and B). Thus, 2W1S:I-A^b-binding T cells that were positively selected by I-A^d/I-E^d and negatively selected by I-A^b were capable of responding to 2W1S, but 7-fold less well on a per cell basis than those that were positively and negatively selected by I-A^b.

The antigen dose used for immunization was reduced to assess the functional avidity of the T cells in the chimeras. The 2W1S:I-A^b+ T cells in F_1 > B6 chimeras increased 34-fold following injection of 1 µg of 2W1S (Fig. 10B). Notably, the cells in F_1 > BALB/c chimeras were also capable of responding to this low dose of 2W1S as evidenced by a 6-fold expansion over the starting number. When the fold expansions were set to 100% at the 50 µg dose, it became clear that antigen dose-response curves for the cells in each population that were capable of expansion were very similar (Fig. 10C). Together, the results lead to 2 conclusions: (i) 5- to 7-fold more of the 2W1S:I-A^b-binding CD4+ T cells that were positively selected on I-A^b were capable of responding to 2W1S than was the population that was selected on I-A^d/I-E^d, and (ii) the functional avidities of the cells that were capable of responding in both populations was similar.

Detection of Naïve Foreign-Peptide:MHC^A-Binding T Cells in Humans Expressing MHC^B

The experiments comparing the T cell repertoires in mice indicated that naive foreign peptide:MHC^A-binding T cells were present in expressing

MHCB hosts. We sought to confirm this conclusion in humans. Magnetic bead enrichment was performed on peripheral blood mononuclear cells (PBMCs) from influenza virus vaccinated people using a tetramer containing the influenza hemagglutinin (HA) peptide 307–319 (86) bound to HLA-DR4 (DR4).

All vaccinated individuals who expressed DR4 contained a $CD45RA^{low}$ HA:DR4-binding CD4+ T cell population at a frequency of about 140 cells per million CD4+ T cells (Fig. 11A and B). The lack of CD45RA (Fig. 11A) suggested that these were the memory cell progeny of naive cells that had responded to the vaccine (105). DR4+ individuals also had much smaller (6 cells per million CD4+ T cells) populations of $CD45RA^{high}$ naive HA:DR4-binding CD4+ T cells (Fig. 11A and B). These cells may not have been activated because they did not enter the draining lymph nodes during the time that the vaccine antigen was presented there. HA:DR4 tetramer binding to both $CD45RA^{low}$ and $CD45RA^{high}$ CD4+ populations was TCR-specific, as it bound to less than 1 cell per million CD8+ T cells (Fig. 11A and B).

Remarkably, $CD45RA^{high}$ naive HA:DR4-binding CD4+ T cells were detected in most DR4+ individuals at a similar frequency (5 cells per million total CD4+ cells) as in DR4+ individuals (Fig. 11A and B). In contrast to DR4+ individuals, DR4- individuals had very few $CD45RA^{low}$ HA:DR4-binding CD4+ memory T cells despite having been vaccinated (Fig. 11A and B). This finding could have been related to the fact that the antigen-presenting cells in DR4- individuals do not express DR4, and thus would be incapable of presenting the DR4-restricted HA peptide after vaccination. In any case, the presence of naive phenotype HA:DR4-binding CD4+ T cells in people lacking DR4 indicated that positive selection on DR4 was not absolutely required for the generation of this population.

Discussion

The presence of 2W1S:I-A^b-binding T cells in I-A^b- mice and HA:DR4-binding T cells in DR4- individuals would appear to be at odds with the theory of positive selection. However, several pieces of evidence indicated that these T cells differed from the 2W1S:I-A^b-binding T cells in B6 mice or HA:DR4-binding T cells in DR4+ individuals. First, the unlawful 2W1S:I-A^b-binding T cells in BALB/c mice or HA:DR4-binding T cells in DR4- individuals did not become activated following injection of 2W1S or HA. This finding could have been related to the fact that these peptides cannot bind to I-A^d/I-E^d or non-DR4 HLA molecules. Alternatively, 2W1S:I-A^d/I-E^d or HA:non-DR4 complexes may have formed but were unrecognizable by 2W1S:I-A^b- or HA:DR4-binding T cells. Thus, unlike the 2W1S:I-A^b- or HA:DR4-binding T cells in B6 mice or DR4+ people, the 2W1S:I-A^b- or HA:DR4-binding T cells in BALB/c mice or DR4- humans were not useful participants in the immune responses to these peptides.

The second piece of evidence indicating that the 2W1S:I-A^b-binding T cells in BALB/c mice differed from those in B6 mice related to fine specificity. The finding that the number of 2W1S:I-A^b-binding cells in F_1 > BALB/c chimeras was 5-fold lower than the number in intact BALB/c hosts indicated that many of the cells in BALB/c mice were also specific for unknown self-peptide:I-A^b complexes and would have been deleted in an I-A^b-expressing thymus. Huseby et al. (46) described similar cells in transgenic mice expressing a single self-peptide:MHC complex. These cells recognized peptides bound to many allelic forms of MHC and were tolerant of many TCR contact residue substitutions in the peptide. The absence of these peptide:MHC degenerate/promiscuous clones in normal hosts indicates that although they may be positively selected, they are then

normally removed by negative selection via recognition of a diverse set of self peptide:MHC ligands.

Because many of the 2W1S:I-A^b-binding T cells in BALB/c mice were also specific for unknown self-peptide:I-A^b complexes, they could be thought of as alloreactive T cells. It should be noted, however, that these cells did not show signs of activation following injection of F_1 spleen cells that were not pulsed with 2W1S peptide. Thus, it is possible that the self-peptide:I-A^b complexes that caused the deletion of such cells in F_1 > BALB/c chimeras were different from those displayed by B6 spleen cells. Alternatively, the TCRs on these cells may have had a high enough affinity for certain self-peptide:I-A^b complexes to cause deletion of immature T cells but not high enough to activate mature cells as described in another system (134).

Notably, some foreign-peptide:I-A^b-binding naive CD4+ T cells remained in F_1 > BALB/c chimeras. This finding indicates that some genuine foreign-peptide:I-A^b-specific, self-peptide:I-A^b tolerant T cells can be positively selected by I-A^d and/or I-E^d. The alternative explanation that these clones were positively selected by I-A^b molecules expressed on the F_1 bone marrow derived cells was ruled out by earlier work showing bone marrow-derived cells cannot mediate positive selection of CD4+ T cells (135). However, it is important to note that the 2W1S:I-A^b-binding populations in F_1 > BALB/c chimeras were 5-times smaller than the comparable ones in F1 > B6 chimeras. Thus, positive selection on self-MHC (in this case defined as the I-A^b of the tetramer) had a beneficial effect on naive population size. This effect was smaller than the 40- to 600-fold effects observed in classic experiments by Bevan (31) and Sprent (125) for cytotoxic and helper T cell responses in immunized mice.

The discrepancy was explained by our finding that a smaller fraction of the 2W1S:I-A^b-binding population in F_1 > BALB/c mice responded to antigen injection compared to the comparable population in F_1 > B6 mice. Notably, the responsive cells in both groups had the same functional avidity. These results are consistent with the possibility that the 40 naive 2W1S:I-A^b tetramer-binding cells in F_1 > BALB mice contained a small subpopulation that responded to 2W1S:I-A^b with exactly the same sensitivity as the majority of cells in F_1 > B6 mice, and a larger subpopulation that did not respond even at the highest dose of antigen. Therefore, although positive selection on MHC^A was not absolutely required to produce foreign-peptide:MHC^A-binding clones, it had a large effect on selecting responsive clones.

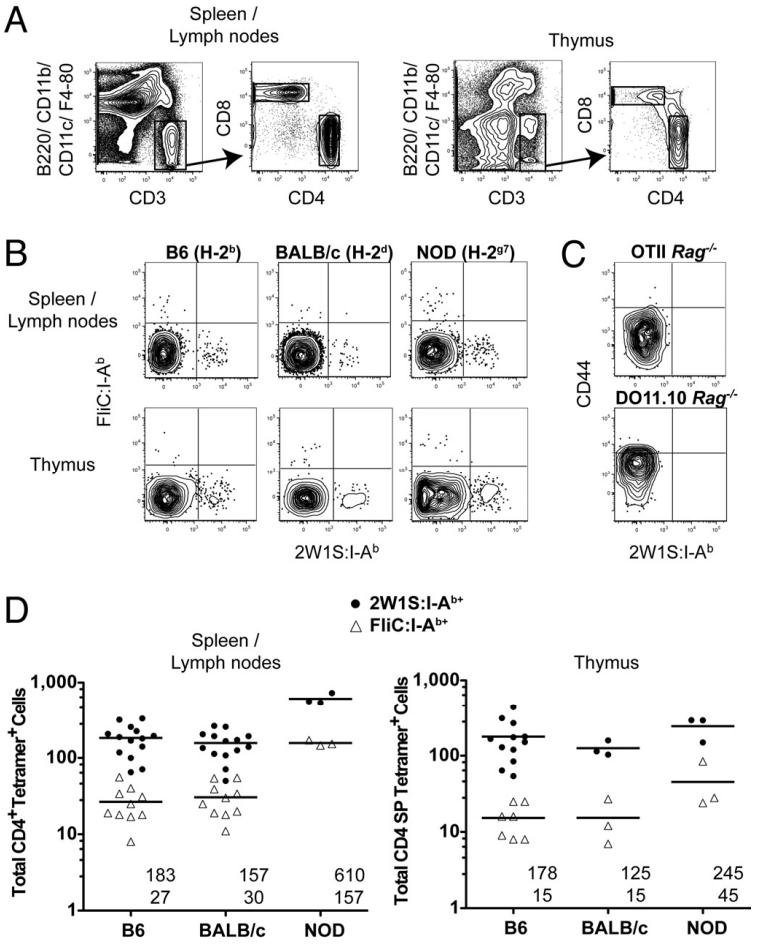

Figure 7. Detection of naive foreign-peptide:MHC^{A}-binding T cells in mice expressing MHC^{B}. A, Gates used to identify T cells in peptide:I-A^{b} tetramer-enriched spleen and lymph node or thymus samples. T cells were identified as CD3+ B220- CD11b- F4/80- CD11c events (left), which were further gated into CD4+ and CD8+ populations (right). **B,** FliC:I-A^{b} tetramer versus 2W1S:I-A^{b} tetramer staining for CD4+ T cells from 2W1S:I-A^{b} and FliC:I-A^{b} tetramer-enriched spleen and lymph node or thymus samples from naive mice. **C,** CD44 versus 2W1S:I-Ab tetramer staining on CD4+ T cells from 2W1S:I-A^{b} tetramer-enriched spleen and lymph node samples of an OTII *Rag-1-/-* or a DO11.10 *Rag-1-/-* TCR transgenic mouse. **D,** Total CD4+ 2W1S:I-A^{b}+ (circles) or FliC:I-A^{b}+ (triangles) cells from the spleen and lymph nodes (Left) or thymus (Right) of individual mice with the mean values for each group indicated as horizontal bars and numerically under each set of values (upper: 2W1S:I-A^{b}; lower: FliC:I-A^{b}).

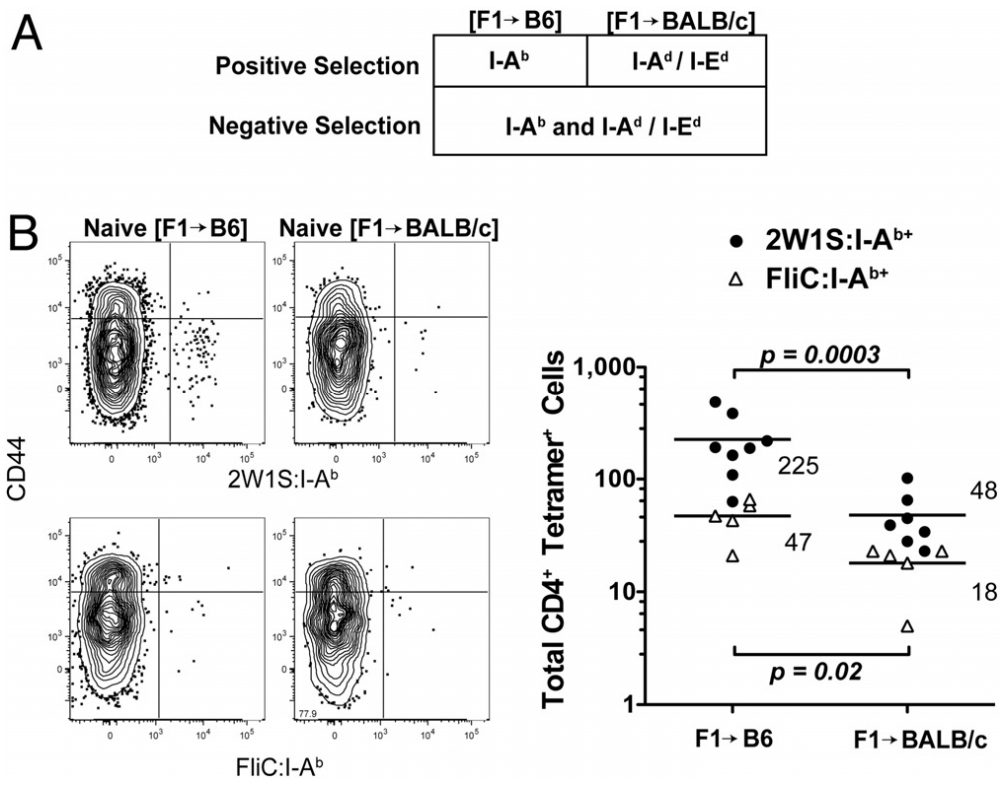

Figure 8. Foreign-peptide:I-A^b-specific T cell populations in F_1 > parent chimeras. **A,** Summary showing the MHCII molecules responsible for positive and negative selection of CD4+ T cells in F_1 > parent chimeras. **B,** CD44 versus 2W1S:I-A^b (upper) or FliC:I-A^b (lower) tetramer staining for CD4+ T cells from the spleen and lymph nodes of a naive F_1 > B6 (left) or F_1 > BALB/c (right) chimera and total CD4+ 2W1S:I-A^b+ (circles) or FliC:I-A^b+ (triangles) cells from the spleen and lymph nodes of individual F_1 > B6 or F_1 > BALB/c chimeras with the mean values for each group indicated as horizontal bars. *P* values are indicated on the plot.

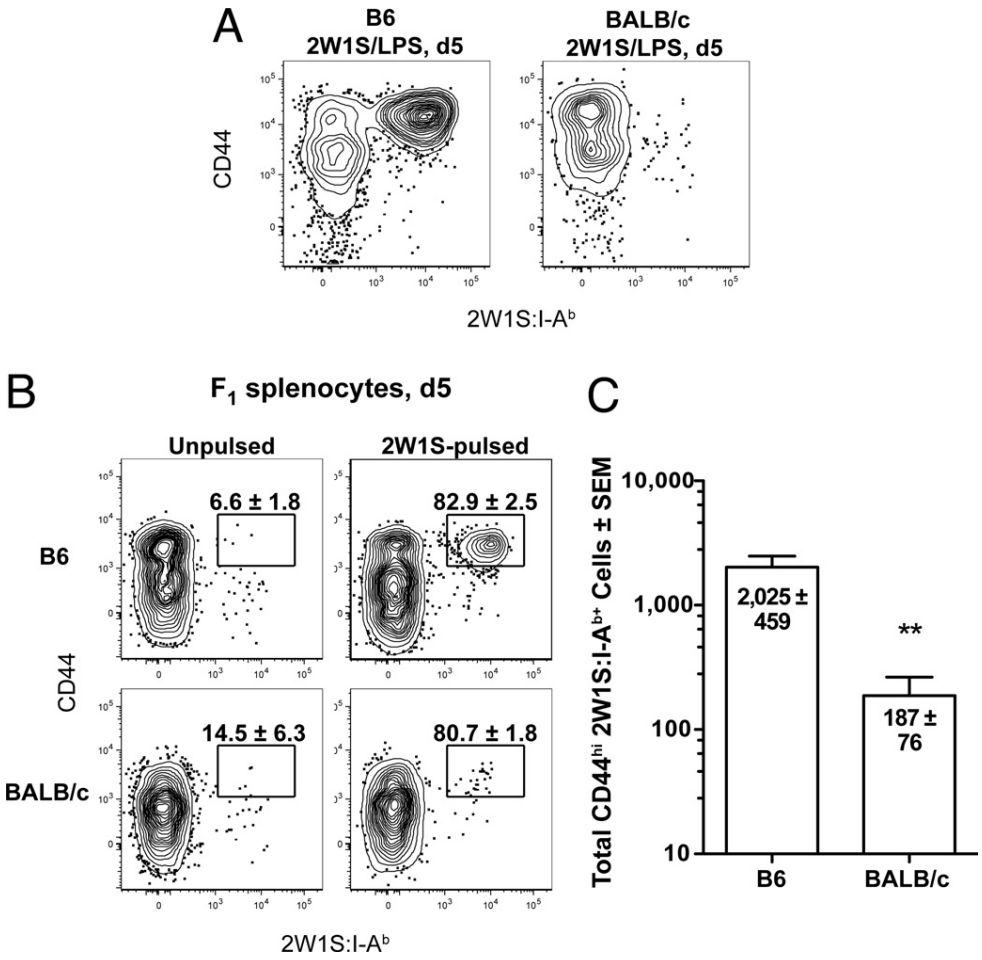

Figure 9. Foreign-peptide:I-A^b-specific T cell populations in BALB/c mice are less functional than those in B6 mice. A, CD44 versus 2W1S:I-A^b tetramer on CD4+ T cells from 2W1S:I-A^b tetramer-enriched spleen and lymph node cells from a B6 (left) or BALB/c (right) mouse 5 days after i.v. injection of 50 µg 2W1S peptide and 5 µg LPS. **B,** CD44 versus 2W1S:I-A^b tetramer plots as in ***A*** from a B6 (upper) or BALB/c (lower) mouse 5 days after i.v. injection of unpulsed (left) or 2W1S peptide-pulsed F_1 splenocytes (right). The mean percentage (± SEM, $n = 3$) of CD44^{high} cells in the 2W1S:I-A^b+ population is indicated on each plot. **C,** Mean CD44^{high} 2W1S:I-A^b+ cells (± SEM, $n = 3$) from B6 or BALB/c mice 5 days after i.v. injection of 2W1S peptide-pulsed F1 splenocytes. **, $P = 0.01$.

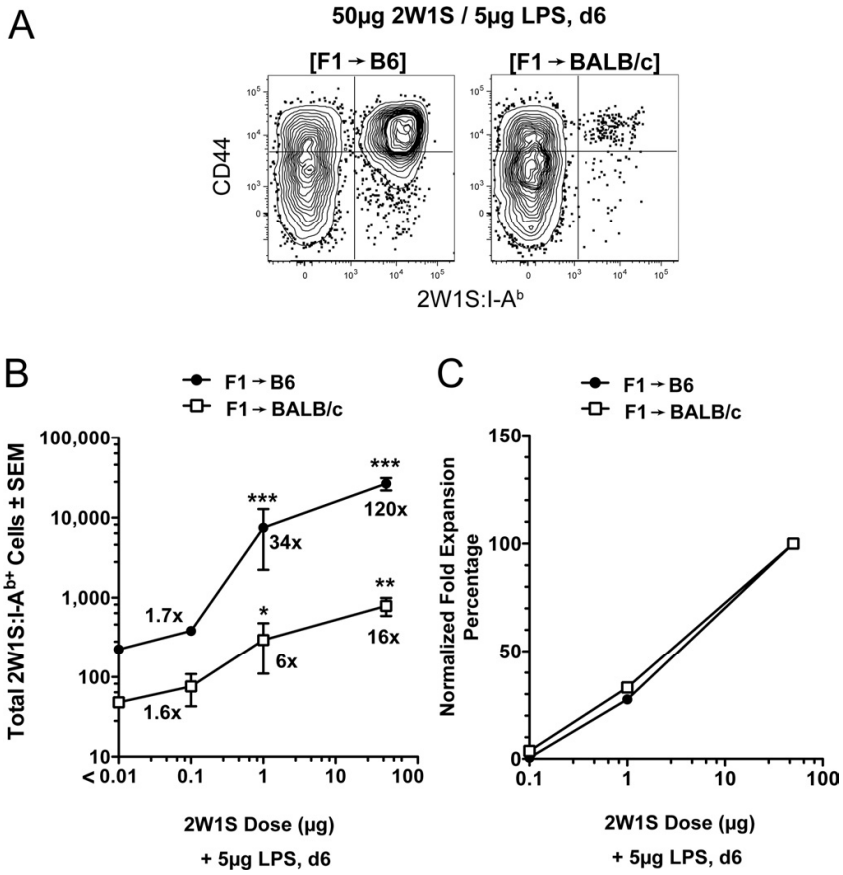

Figure 10. 2W1S:I-A^b-specific T cell populations in F_1 > BALB/c chimeras are less functional than those in F_1 > B6 chimeras. A, CD44 versus 2W1S:I-A^b tetramer on CD4_ T cells from 2W1S:I-A^b tetramer-enriched spleen and lymph node cells from a F_1 > B6 (left) or F_1 > BALB/c (right) mouse 6 days after i.v. injection of 2W1S peptide and LPS. **B,** Mean CD4+ 2W1S:I-A^b+ cells (± SEM, n = 3 at each dose) from F_1 > B6 (filled symbols) or F_1 > BALB/c (open symbols) chimeras 6 days after i.v. injection of the indicated amounts of 2W1S peptide and LPS. Values that are significantly greater than the naive values are indicated by asterisks: ***, P = 0.001; **, P = 0.01; *P = 0.05. The numbers near each data point represent the fold increase of CD4+ 2W1S:I-A^b+ cells calculated by dividing the mean number of CD4+ 2W1S:I-A^b+ cells from immunized mice by the mean number of CD4+ 2W1S:I-A^b+ cells from the naive chimeras shown in Fig. 2. **C,** Normalized fold expansion percentage values = [(mean number at indicated dose - mean naive number)/(mean number at 50 µg dose - mean naive number)] x 100.

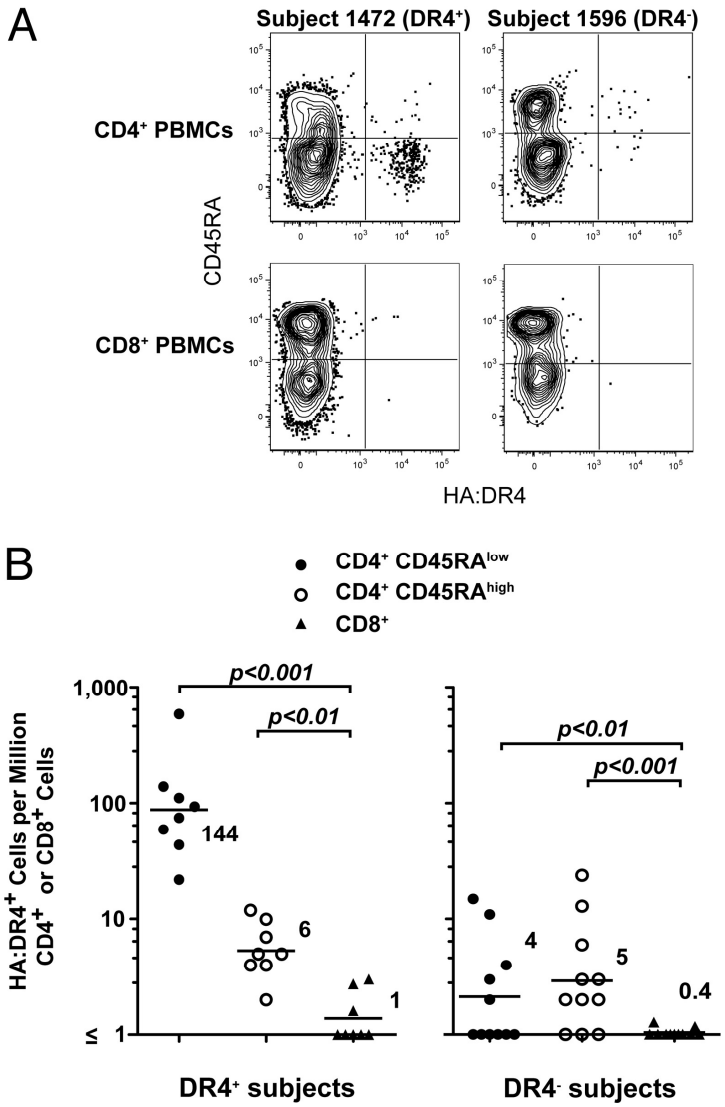

Figure 11. Detection of naive foreign-peptide:MHC^{A}-binding T cells in humans expressing MHC^{B}. A, Contour plots of CD45RA versus HA:DR4 tetramer fluorescence intensity for CD19- CD4+ (upper) or CD8+ (lower) cells from tetramer-enriched samples from a subject who expresses DR4 (left) or a different subject who expresses non-DR4 alleles (Right), 1 year after influenza virus vaccination. **B,** The number of CD45RA^{low} (filled circles) or CD45RA^{high} (open circles) CD4+ tetramer+ cells per million total CD4+ T cells and CD8+ tetramer+ cells per million total CD8+ T cells (triangles). The mean values indicated as horizontal bars are shown for each group.

CHAPTER 5

The large size of a peptide-MHCII-specific naïve CD4+ T cell population is associated with particular TCR contact residues

T cells expressing $\alpha\beta$ antigen receptors (TCR) recognize peptides embedded in major histocompatibility complex (MHC) molecules (pMHC) displayed by antigen-presenting cells (APCs) (24, 123). The genes encoding each TCR chain are randomly rearranged products composed of V, (D), and J gene segments (14). During T cell development, clones that express non-functional TCRs or TCRs with high affinity to self-pMHC are eliminated in the thymus. Surviving clones populate the secondary lymphoid organs and form a naïve T cell repertoire that contains a collection of diverse TCRs each specific for one of several hundred thousand foreign-pMHC (14).

Recently, our laboratory and others directly measured the frequencies of different foreign pMHC specific populations in the naïve repertoire and demonstrated that their population sizes vary (127-130). For example, we found that B6 mice contained 200 naïve CD4+ T cells specific for one peptide:I-A^b ligand but only 20 cells specific for another (127, 136). Differences in naïve population size were found to account for the magnitude and TCR diversity observed in immune responses to different peptides. Therefore, the advantage provided by large naive population size could contribute to the phenomenon of immunodominance. Other studies showed that small naïve populations were at risk for extinction as the naïve T cell repertoire contracts during aging (137, 138).

What mechanism(s) control the size of individual pMHC-specific populations in a naïve T cell repertoire? Thymic selection is one possibility. Developing thymocytes express randomly generated TCRs at the CD4+ CD8+ double positive stage of development (30). Only those cells expressing TCRs with low affinity for self-pMHC ligands displayed on the thymic cortical epithelium receive survival signals and become positively selected. Our recent findings show that positive selection by self-pMHC

optimizes the absolute number of clones specific for foreign peptides bound to the same MHC molecule (136). Since multiple self-pMHC complexes can cause the positive selection of the same foreign-pMHC-specific population (34-36), it is possible that certain foreign-pMHC-specific naïve populations are large because of a capacity to be positively selected by a large set of self-pMHC ligands. It is also possible that size differences between naïve pMHC-specific populations are caused by negative selection. For example, a foreign-pMHC-specific naive population may be small because many of its members are deleted due to high affinity cross reaction with a self-pMHC.

The structure of the pMHC might also influence the size of the corresponding naïve T cell population. Several groups have shown that MHCI-bound influenza peptides with prominent TCR contact residues are recognized by very diverse but not necessarily large naïve CD8+ T cell populations (139-141). In addition, Stewart-Jones et al. (142) demonstrated that an influenza peptide with featureless TCR contact residues could adjust its conformation to accommodate interaction with several TCRs. We found that large naïve CD4+ T populations contained more TCR Vβ chains than small populations (127), indicating that large population size was a consequence of a pMHCII being recognizable by many diverse TCRs. Therefore, although the “rules” are far from being understood, it is likely that the topology of a given MHC-bound peptide influences the size of the naïve T cell population that can recognize it.

In this chapter, we used to a sensitive pMHCII-tetramer based enrichment method to test the mechanisms that regulate the size of CD4+ naïve T cell populations. Our results show that large and diverse naïve CD4+ T cell populations tend to recognize MHCII-bound peptides with certain TCR contact residues. Thus, in the same way that certain amino

acids favor the binding of peptides to MHC, so do some amino acids favor the binding of peptides to the TCR.

Perturbation of Positive Selection Does Not Alter the Relationship Between Large and Small Naïve CD4+ T Cell Populations

We studied naïve CD4+ T cells specific for two different I-A^b-binding foreign peptides. One of the peptides called 2W (formerly 2W1S (101, 127, 136)) is a variant of peptide 52-68 from the I-Eα chain and contains the I-A^b binding nonamer core AWGALANWA. The other peptide comprised amino acids 427-441 from the FliC flagellar protein of *Salmonella typhimurium* (103) and contains the I-A^b binding nonamer core FNSAITNLG. Previously, we produced 2W:I-A^b and FliC:I-A^b tetramers and used them with magnetic bead enrichment to show that individual B6 mice contain about 200 2W:I-A^b- and 25 FliC:I-A^b-binding naïve CD4+ T cells in the spleen and lymph nodes (127, 136).

We first determined whether impairment of thymic positive selection would equalize the size of these populations. Positive selection was perturbed by manipulating the thymic epithelium in radiation bone marrow chimeras. B6 bone marrow cells were transferred to lethally irradiated *H2-DMa-/-* mice (143-145) or YAe (146, 147) single peptide mice (SP), which were engineered to express only CLiP:I-A^b or Ea:I-A^b. The radio-resistant thymic epithelium in these B6 > SP chimeras only expresses either CLiP:I-A^b or Ea:I-A^b, while B6 bone marrow-derived thymic dendritic cells display a diverse set of self-pMHCII. Positive selection of CD4+ T cells is impaired in these chimeras because self-peptide-MHCII diversity is required for this process to operate efficiently (145-149).

Double tetramer-based enrichment was then performed on thymocytes from individual B6 > SP chimeras or normal B6 mice as

controls. As shown in Fig. 12A, B6 mice contained mutually exclusive naïve populations in the thymus that bound either the 2W:I-A^b tetramer or the FliC:I-A^b tetramer. The vast majority of cells that bound either tetramer were CD4+ CD8-. Individual B6 mice had on average 164 2W:I-A^b+ CD4+ CD8- thymocytes and 18 FliC:I-A^b+ cells [Fig. 12B, (136)]. Only about 5 2W:I-A^b+ or FliC:I-A^b+ CD4- CD8+ thymocytes were detected in each mouse. This level of 5 cells per mouse was considered to represent background binding, since CD8+ T cells should not bind pMHCII ligands via the TCR. Both the 2W:I-A^b-specific and the FliC:I-A^b-specific CD4+ CD8- thymocyte populations were significantly larger than the 5 cell limit of detection. As expected because of the reduction in total thymocytes due to impaired positive selection (Fig. 12C), the 2W:I-A^b+ CD4+ CD8- population fell to an average of 8 cells per mouse in B6 > SP chimeras, which was barely but significantly above the limit of detection (Fig. 12B). However, the total number of FliC:I-A^b+ CD4+ CD8- thymocytes was even lower, falling below the limit of detection in 5 of 7 mice (Fig. 12B). Therefore, although impairment of positive selection greatly reduced the absolute number cells in each population, the greater size of the 2W:I-A^b-specific population was maintained under this condition.

Perturbation of Negative Selection Does Not Alter the Relationship Between Large and Small Naïve CD4+ T Cell Populations

It was also possible that thymic negative selection on self-pMHCII accounted for the difference in the size of 2W:I-A^b- and FliC:I-A^b-specific CD4+ naïve T cell populations. Before assessing this possibility, we first confirmed that the pMHCII tetramer-based enrichment method had the sensitivity to detect clonal deletion of T cells specific for a genuine self-pMHCII. The peptide in the tetramer used for this purpose consisted of

amino acids 376-391 from the IgM heavy chain constant region, which was identified by Rudensky and colleagues as an abundant I-A^b-bound self-peptide (150). An IgM:I-A^b tetramer was generated and used to enumerate IgM:I-A^b-specific T cells. Individual thymii from B6 mice contained 6 ± 4 IgM:I-A^b+ CD4+ CD8- cells (Fig 13A and B), which was at the detection limit of the enrichment method. In contrast, mice lacking IgM (*μ*MT or *JH-/-* mice) contained about 40 IgM:I-A^b+ CD4+ CD8- cells per thymus (Fig 13A and B). The most likely explanation for the presence of IgM:I-A^b+ cells in *μ*MT or JH-/- mice but not B6 mice was clonal deletion in the latter strain.

We next enumerated pMHCII-specific populations in K14-$A^b\beta$ mice in which negative selection is impaired. The impairment in these mice comes about because I-A^b MHCII molecules are expressed by cortical epithelial cells allowing for positive selection of CD4+ T cells, but not medullary epithelial cells and bone marrow derived cells, which play essential roles in clonal deletion (133, 135, 151, 152). The T cell repertoire in these mice is therefore enriched for self-pMHCII-specific CD4+ T cells (152, 153).

Accordingly, the number of IgM:I-A^b+ CD4+ CD8- thymocytes was at least 50-fold higher in K14-$A^b\beta$ mice than in B6 or IgM-deficient mice (Fig. 13A and B). The finding that more IgM:I-A^b+ CD4+ CD8- thymocytes were present in K14-$A^b\beta$ mice than in IgM-deficient mice suggested that the pre-selection repertoire of a normal B6 mouse contains thymocytes with high affinity for IgM:I-A^b alone, which appear in IgM-deficient mice, and others with high affinity for IgM:I-A^b and another self-pMHCII, which appear in K14-$A^b\beta$ mice. The notion that the cells that were spared deletion in the K14-$A^b\beta$ mice were cross-reactive with respect to peptide specificity was supported by the finding some cells in these mice bound to IgM:I-A^b and 2W:I-A^b (Fig. 13A). This level of cross-reactivity raised the possibility that

some cells with 2W:I-A^b or FliC:I-A^b specificity might also be deleted in B6 mice due to cross-reactivity on unknown self-pMHCII. Less deletion of this type could have explained why the 2W:I-A^b-specific population was larger than the FliC:I-A^b-specific population.

Indeed, the numbers of 2W:I-A^b+ and FliC-I:A^b+ cells in the thymus in K14-$A^b\beta$ mice were at least 10-fold higher than in B6 mice (Fig. 13C). Despite the elevation in the absolute number of both populations, the 2W:I-A^b-specific population was still larger than the FliC:I-A^b-specific population in every animal tested. Similar results were obtained in bone marrow chimeras generated by reconstituting lethally irradiated B6 hosts with bone marrow cells from *H2-DMa-/-* or YAe mice (SP > B6) (Fig. 13C), in which negative selection was impaired because only CLiP:I-A^b or Ea:I-A^b complexes were expressed by bone marrow-derived cells. Together the results show that while impairment of thymic selection increased the absolute numbers of both populations, the 2W:I-A^b-specific population was still larger than the FliC:I-A^b-specific one.

The Large Size of the 2W:I-A^b-Specific Population is Associated with Its Specific TCR Contact Residues

The finding that the hierarchy between the 2W:I-A^b+ and the FliC:I-A^b+ populations was not altered by perturbation of thymic selection suggested that a structural difference in the peptides might be responsible. One possible difference was I-A^b binding capacity (154). If the 2W peptide bound I-A^b better than FliC it could form a more stable complex for TCR binding. We measured the size of the naïve cell population specific for a peptide that is closely related to 2W called 3K (101, 155) to address this possibility. The 3K peptide has the same MHC anchor residues as 2W but differs at the TCR contact residues at amino acid positions P2, P3, P5 and

P8 (Fig. 14A). If the 2W:I-A^b-specific naïve cell population was relatively large solely because of its MHC anchor residues, and presumably its ability to bind I-A^b, then the 3K:I-A^b-specific population should have been equally large. In fact, the population of 3K:I-A^b-specific cells in the spleen and lymph nodes or thymus was 7-9-fold smaller than the 2W:I-A^b-specific population (Fig. 14B and C). This result suggested that the capacity of I-A^b-bound 2W peptide to be recognized by a large naïve population was not solely related to its MHC anchor residues.

This finding pointed toward something special about the TCR contact residues in the 2W peptide. Based on analogy to the crystal structure of the 3K:I-A^b complex (PDB code: 1LNU, (155)) (data not shown), the sidechains from the tryptophan (Trp) residues at P2 and P8 of the 2W peptide are likely to contribute significantly to the solvent exposed surface available for TCR binding. We therefore produced several tetramers containing 2W variant peptides in which the Trp residues at positions P2 were changed to glycine (Gly) (1G) or arginine (Arg) (1R) or the Trp residues at positions P2 and P8 were both changed to Gly (2G) to test for the role of these positions in the large size of the 2W:I-A^b-specific population (Fig. 15A). Each of the 2W variant peptides bound to I-A^b with the same efficiency as the parent 2W peptide based on the capacity to compete with a reference peptide for I-A^b binding *in vitro* (Fig. 15B). The tetramers were then used to identify naïve CD4+ T cell populations. As shown in Fig. 15C, defined populations of naïve CD4+ T cells specific for each of the three 2W variant:I-A^b complexes were detected in B6 mice. Eighty to 95% of the naïve CD4+ T cells identified by each of the 2W variant:I-A^b tetramers failed to bind the 2W:I-A^b tetramer. This lack of cross reactivity is consistent with P2 and P8 being important TCR contacts, which when changed, were bound by different T cell populations.

Importantly, the CD4+ populations specific for the 1G and 1R variants were 3-fold smaller than the 2W:I-A^b-specific population, while the population specific for the 2G variant was 6 times smaller (Fig. 15D). This hierarchy (2W > 1G = 1R > 2G) was also observed for expanded populations present 6 days after intravenous injection of 50 μg of the relevant peptide plus lipopolysaccharide (LPS) (Fig. 16A). Because earlier work (127) showed that naïve population size predicts the size of effector cell populations generated by peptide injection, this finding supports the accuracy of the naïve population numbers obtained by analysis of unprimed mice. Collectively, these results are consistent with the hypothesis that the Trp TCR contact residues in the 2W peptide contributed to the large size of the 2W:I-A^b-specific T cell population.

We next tested the hypothesis that the 2W:I-A^b-specific population was larger than those specific for the 2W variant:I-A^b populations because of recognition by more TCR Vβ chains. The TCR Vβ chain usage of 2W:I-A^b- and 1G:I-A^b-specific populations was examined in B6 mice immunized with these peptides. As reported previously (127), the 2W:I-A^b-specific population consisted of T cells that utilized all 14 TCR Vβ chains tested. On the contrary, T cells using Vβ 5.1/5.2, Vβ 9, Vβ 10b, or Vβ 11 chains were absent in the 1G:I-A^b-specific population, while the percentage of Vβ 2, Vβ 8.3 and Vβ 12-expressing T cells was twice that of the 2W:I-A^b-specific population (Fig. 16B). Taken together, these results indicated that the 2W:I-A^b-specific population contained a larger and more diverse set of clones than those specific for 1G:I-A^b.

Tryptophan Residues at TCR Contact P2 Increase pMHCII-Specific Naïve T Cell Population Size

The results suggested that the presence of Trp as a TCR contact residue at P2 of the 2W peptide allowed recognition by more TCRs. If this was correct, then substitution with Trp at P2 of peptides that are normally recognized by small naïve T cell populations should result in a pMHCII that is recognized by a larger naïve population. To test this hypothesis, we first generated two tetramer containing variants of the FliC peptide with Trp substitutions at P2 alone ($FliC_{1W}$) or P2 and P8 ($FliC_{2W}$) (Fig 17A). These FliC variant peptides had the same I-A^b binding efficiency as the FliC parent peptide (Fig 17B). When tetramer enrichment was performed in individual B6 mice, 2-fold and 4-fold more T cells were detected in the spleen and lymph nodes by the $FliC_{1W}$:I-A^b and the $FliC_{2W}$:I-A^b tetramers, respectively, than were detected by the FliC:I-A^b tetramer (Fig 17C). These tetramer binding populations were mutually exclusive (data not shown), indicating that the Trp residues in P2 and P8 positions altered the topology of FliC:I-A^b epitope, leading to the binding of the FliC-variant tetramer to a completely different yet larger set of T cells. Moreover, the hierarchy of T cell numbers in expanded populations present 6 days after intravenous injection of 50 µg of the relevant peptide plus LPS matched that of the naïve populations ($FliC_{2W}$> $FliC_{1W}$>FliC) (Fig. 17D). These results added further evidence to the contention that Trp residues at the P2 TCR contacts fostered recognition by more T cells in the naïve repertoire.

To rule out the possibility that the FliC results were the result of chance, the Trp substitution experiment was performed with a different peptide. The chicken ovalbumin peptide 329-337 was chosen for this purpose. This is a well-studied peptide recognized by CD4+ T cells from the OT-II TCR transgenic line (107, 156). A disulfide trap strategy was used to tether the peptide to the I-A^b alpha chain to alleviate concerns about it binding in the incorrect register (156). A cysteine (Cys) substitution

was made at position 72 of the I-A^b alpha chain construct used for tetramer production. In addition, new constructs were produced in which OVA329-337 (OVAC, Fig. 18A) or its P2 Trp substituted variant ($OVAC_{1W}$) was followed by a Gly and Cys residue and linked to the I-A^b beta chain. A disulfide bond would be expected to form in the transfected insect cell line between the substituted Cys residue in the I-A^b alpha chain and the one just after the peptide, in effect locking the peptide into the correct binding register (157). Tetramers were produced from these constructs and used to detect naïve CD4+ T cells in unimmunized B6 mice. The $OVAC_{1W}$:I-A^b tetramer detected a population of 120 naïve CD4+ T cells that was about 3-times larger than population detected by the OVAC:I-A^b tetramer (Fig. 18B). These results confirm those obtained with the FliC:I-A^b tetramers and solidify the conclusion that the presence of a Trp residue at P2 of an I-A^b-binding peptide produces a complex that can be recognized by a relatively large naïve T cell population.

Discussion

By tracking two foreign pMHCII-specific CD4+ T cell populations, we confirmed the important role that self-pMHCII complexes play in shaping the preimmune repertoire. Reduction in the diversity of self-pMHCII on the thymic epithelium reduced the number of 2W:I-A^b and FliC:I-A^b specific naïve T cells by 10-fold. However, the reduction was not absolute in the case of 2W:I-A^b-specific cells suggesting that some members of this foreign pMHCII-specific population could be positively selected by CLiP:I-A^b or Eα:I-A^b. This finding adds further support to the idea that the self-pMHCII that causes the positive selection of a given T cell clone is structurally different from the foreign pMHCII recognized by that clone with high affinity (35, 36). Alternatively, the few 2W:I-A^b-specific T cells that

developed in B6 > SP chimeras could have been positively selected by one of the few self-pMHCII other than CLiP:I-A^b or Ea:I-A^b that are displayed on the thymic epithelium of *H2-DMa-/-* or YAe mice (158). Nevertheless, our data reinforce the idea that a diverse array of self-pMHCII expressed on the thymic epithelium is required for the generation of a full T cell repertoire.

Our results also shed light on the role that negative selection plays in shaping the T cell repertoire. This effect was most clearly seen in the analysis of K14-$A^b\beta$ mice, in which I-A^b molecules are expressed on the thymic epithelium but not bone marrow-derived cells. For example, a self IgM:I-A^b-specific T cell population went from being undetectable in B6 mice, presumably due to clonal deletion, to a population of several thousand cells in the K14-$A^b\beta$ mice. Even more remarkable was the finding that the number of 2W:I-A^b- and FliC:I-A^b-specific cells increased 5-10-fold in K14-$A^b\beta$ or SP > B6 chimeras in which clonal deletion was impaired by a complete or dramatic lack of self-pMHCII diversity. This result suggests that at least 90% of the cells in the normal preselection repertoire that could bind to 2W:I-A^b or FliC:I-A^b could also bind to an unknown self-peptide:I-A^b complex and were deleted for this reason. The fact that some of the cells that were spared in K14-$A^b\beta$ mice could bind to both 2W:I-A^b and IgM:I-A^b is consistent with earlier work showing that many cells in the pre-deletion repertoire are promiscuous with respect to peptide specificity (46).

Despite the clear role of thymic selection in controlling the absolute number of pMHC-specific T cells, perturbation of the positive or negative selection did not change the fact that the 2W:I-A^b-specific population was always larger than the FliC:I-A^b-specific one. Rather, our results suggest that this phenomenon is related to the specific amino acids present at P2

and P8 of this peptide. A TCR binds to a cognate pMHC via interactions between its CDR loops and the side chains of amino acids at P2, P3, P5, and P8 of the peptide (24). Our results suggest that Trp residues at P2 and P8 create a particularly favorable binding surface for many TCRs, which explains why the 2W:I-A^b-specific population is relatively large. This capacity could be related to the ability of the indole ring of Trp to form hydrogen bonds, and hydrophobic and cation-pi stacking interactions with a variety of other amino acids (159, 160). Thus, Trp residues at P2 and P8 may serve as a binding "hotspots" for many TCRs with appropriate residues in the CDR loops. However, the finding that the 2W:1-A^b-specific population was still larger than the $FliC_{2W}$:I-A^b-specific population, despite the presence of Trp residues at P2 and P8 in both peptides suggests that other factors may contribute to this difference. It is possible that the 2W peptide also has a beneficial amino acid at P5, which binds to the CDR3 loops of the TCR Vα and Vβ chains.

An understanding of the rules that favor peptide side chain-TCR interaction could allow prediction of not only which peptides have properly spaced MHC anchor residues but also TCR contact residues that are likely to be recognized relative large naïve T cell populations. This knowledge would make it possible to identify potential immunodominant peptides from pathogens using purely bioinformatic approaches.

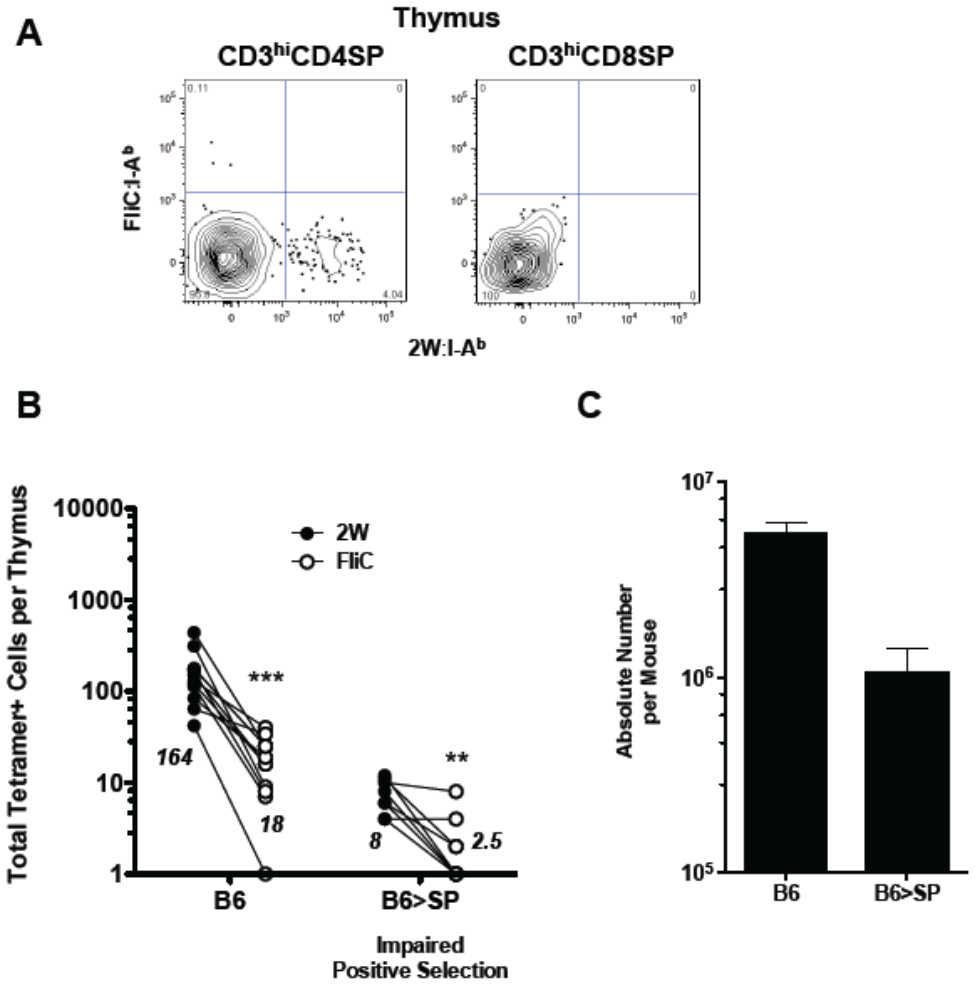

Figure 12. Perturbation of positive selection does not alter the relationship between large and small naïve CD4+ T cell populations. A, Contour plots of FliC:I-A^b tetramer versus 2W:I-A^b tetramer staining for $CD3^{high}$ CD4+ (left) or CD8+ (right) thymocytes from tetramer-enriched thymus samples from naïve B6 mice. **B,** Mean $CD3^{high}$ CD4+ 2W:I-A^b+ (circles) or FliC:I-A^b+ (triangles) cells from thymus samples of individual B6 or B6 > SP chimeras (± SEM, $n > 6$). ***, P-value < 0.001; **, P-value = 0.01. **C,** Mean $CD3^{high}$ CD4+ cells from thymus samples of individual B6 or B6 > SP chimeras (± SEM, $n > 6$). Data are representative of at least 3 independent experiments.

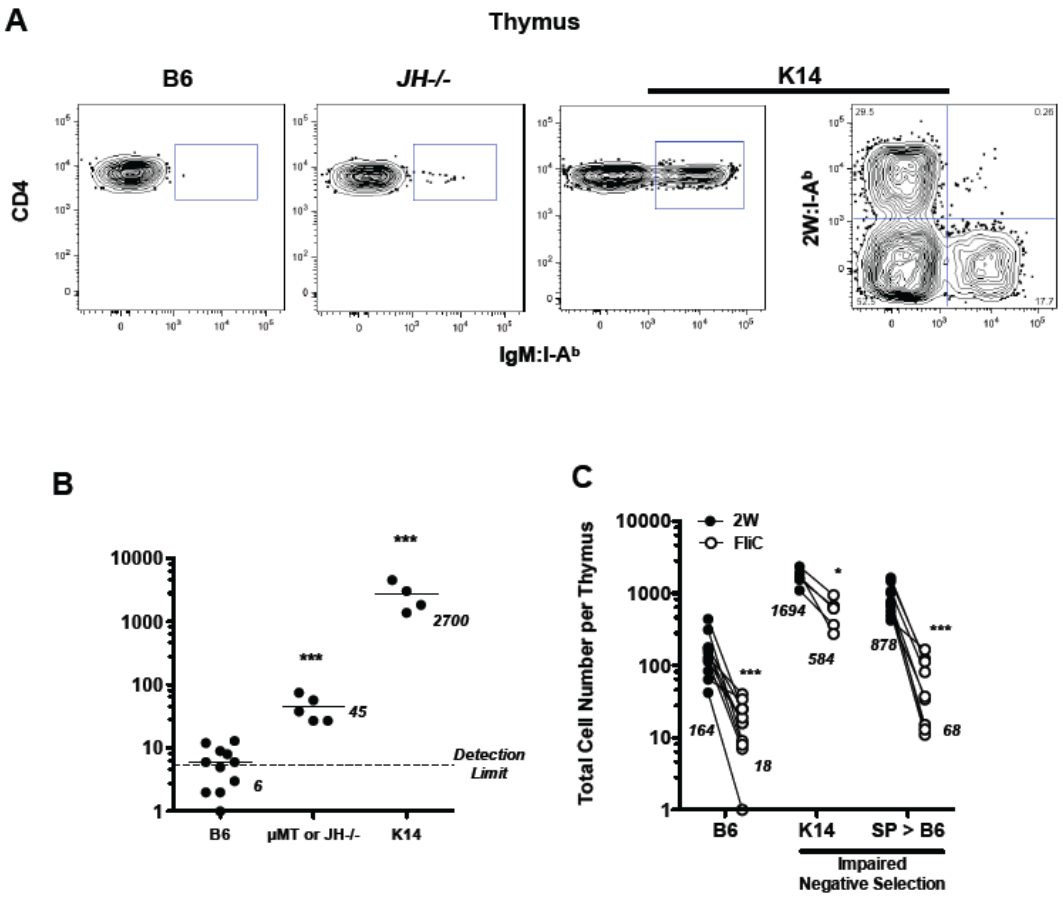

Figure 13. Perturbation of negative selection does not alter the relationship between large and small naïve CD4+ T cell populations. A, Contour plots of CD4 versus IgM:I-A^b tetramer staining for $CD3^{high}$ CD4+ thymocytes from tetramer-enriched thymus samples from naïve B6, μMT or *JH-/-* and K14-$A^b\beta$ mice (left), or 2W:I-A^b tetramer versus IgM:I-A^b tetramer staining for $CD3^{high}$CD4+ thymocytes from tetramer-enriched thymus samples from naïve K14-$A^b\beta$ mice (right). **B,** Total $CD3^{high}$ CD4+ IgM:I-A^b+ cells from thymus samples of individual B6, μMT or *JH-/-* and K14-$A^b\beta$ mice. **C,** Total $CD3^{high}$ CD4+ 2W:I-A^b+ (black circle) and FliC:I-A^b+ (open circle) cells from thymus samples of individual B6 and SP > B6 mice. Mean values for each group are indicated as horizontal bars and numerically under each set of values. Each line connected values from the same individuals. ***, *P*-value < 0.001; *, *P*-value < 0.05. Data are representative of at least 3 independent experiments.

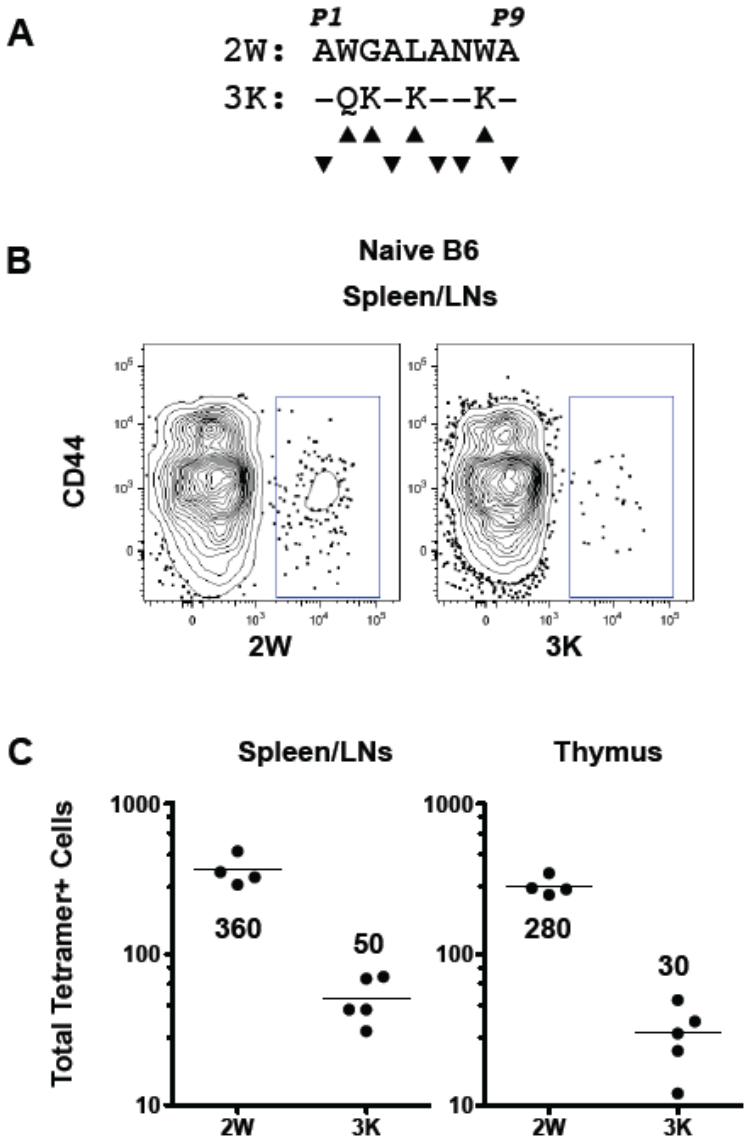

Figure 14. The large size of the 2W:I-A^b-specific population is associated with its specific TCR contact residues. A, The core 9 residues of I-A^b-binding peptide 2W and 3K. **B,** Contour plots of CD44 versus 2W:I-A^b (left) or 3K:I-A^b tetramer staining for CD3+ CD4+ cells from tetramer-enriched spleen and all lymph node samples from naïve B6 mice. **C,** Total CD3+ CD4+ 2W:I-A^b+ and 3K:I-A^b+ cells from spleen and all lymph nodes (left) or thymus (right) samples of individual B6 mice. Mean values for each group are indicated as horizontal bars and numerically under each set of values. Data are representative of at least 3 independent experiments.

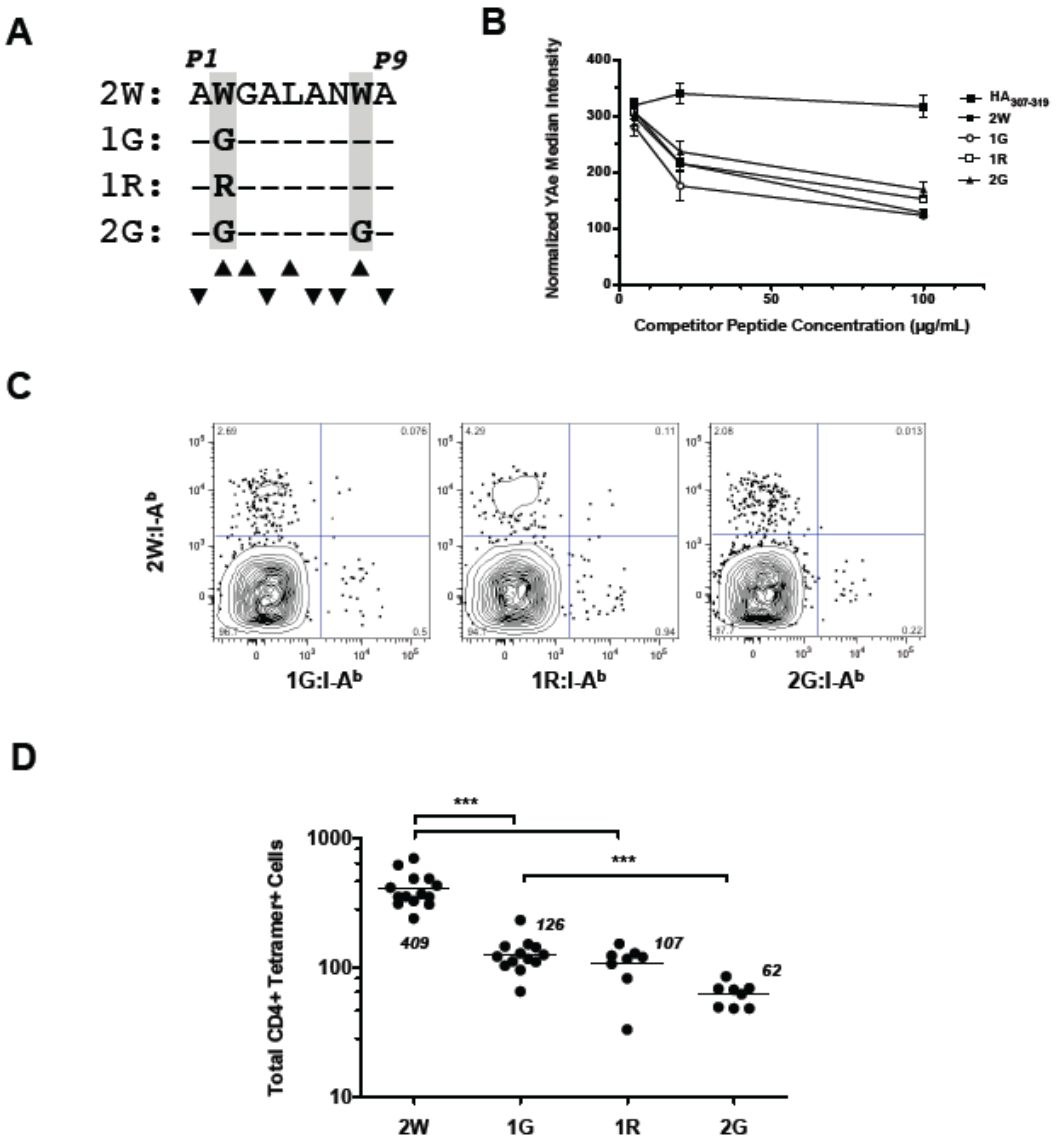

Figure 15. Tryptophan residues at TCR contact P2 and P8 contribute to the large size of the 2W:I-A^b-specific population. A, The core 9 residues of I-A^b-binding peptide 2W and its variants 1G, 1R and 2G. The tryptophan residues and their substitutions at P2 and P8 are highlighted. Respective TCR and MHC contact residues are shown. **B,** Normalized median fluorescence intensities of anti-Ea$_{52-68}$:I-A^b (YAe) staining from B220+ *H2-DMa-/-* spleen after incubation with the Ea$_{52-68}$ peptide plus the indicated concentrations of the control HA$_{307-319}$ peptide or 2W variant peptides. HA$_{307-319}$ (black square), 2W (black circle), 1G (open circle), 1R (open square) and 2G (black triangle). A

reduction in Y-Ae staining indicated that the test peptide out competed the Ea_{52-68} peptide for binding to I-A^b. **C,** Contour plots of 2W:I-A^b versus 1G:I-A^b, 1R:I-A^b or 2G:I-A^b tetramer staining for CD3+ CD4+ cells from tetramer-enriched spleen and all lymph node samples from naïve individual B6 mice. Numbers in the upper right quadrant of each plot represented the mean percent (± SEM, n =3) of the 1G:I-A^b+, 1R:I-A^b+ or 2G:I-A^b+ populations that were also 2W:I-A^b+. **D,** Total CD3+ CD4+ 2W:I-A^b+, 1G:I-A^b+, 1R:I-A^b+ and 2G:I-A^b+ from spleen and all lymph nodes samples of individual B6 mice. Mean values for each group are indicated as horizontal bars and numerically under each set of values. ***, P-value < 0.001. Data are representative of at least 3 independent experiments.

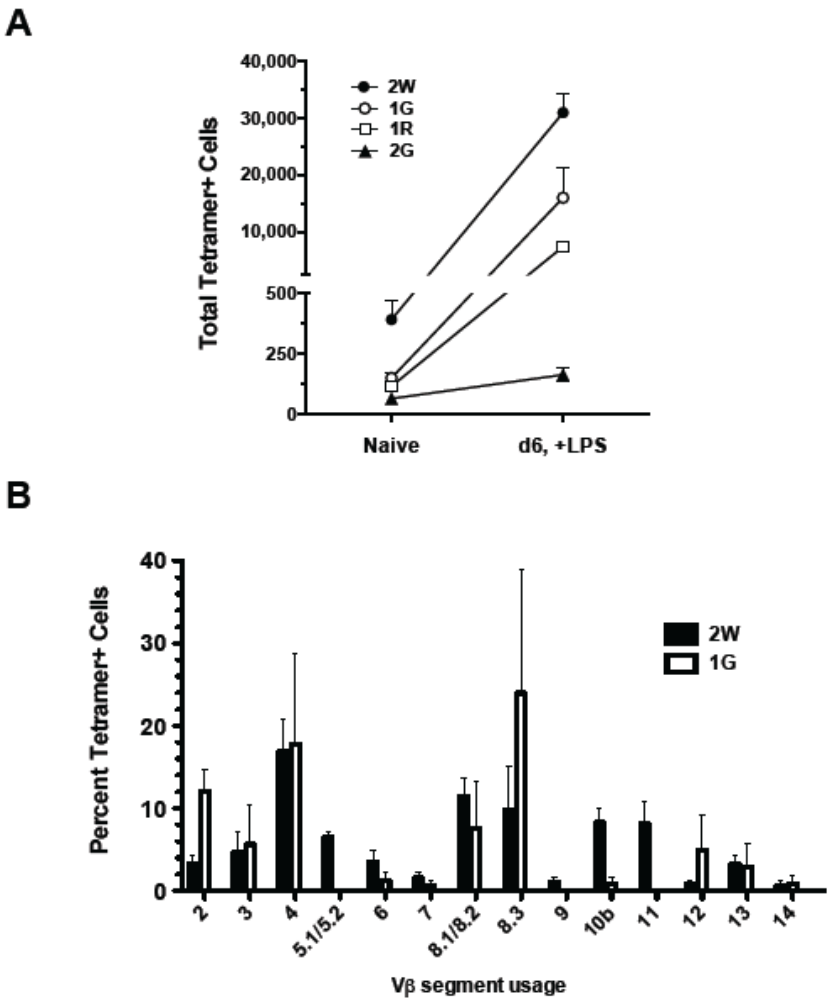

Figure 16. The 2W:I-A^b-specific population contained a larger and more diverse set of clones than those specific for 1G:I-A^b. A, Mean CD3+ CD4+ 2W:I-A^b+, 1G:I-A^b+, 1R:I-A^b+ and 2G:I-A^b+ cells (± SEM, *n* = 3-5) from spleen and all lymph nodes samples of individual B6 mice 6 days after i.v. injection with 50 µg of the relevant peptide plus 5 µg LPS. **B,** TCR Vβ gene segment usage in CD3+ CD4+ 2W:I-A^b+ (filled bar) or 1G:I-Ab+ (open bar) cells from spleen and all lymph nodes samples of B6 mice 6 days after i.v. injection with 50 µg relevant peptide plus 5 µg LPS. Data are mean values + SEM from 2 mice per group. Data are representative of at least 2 independent experiments.

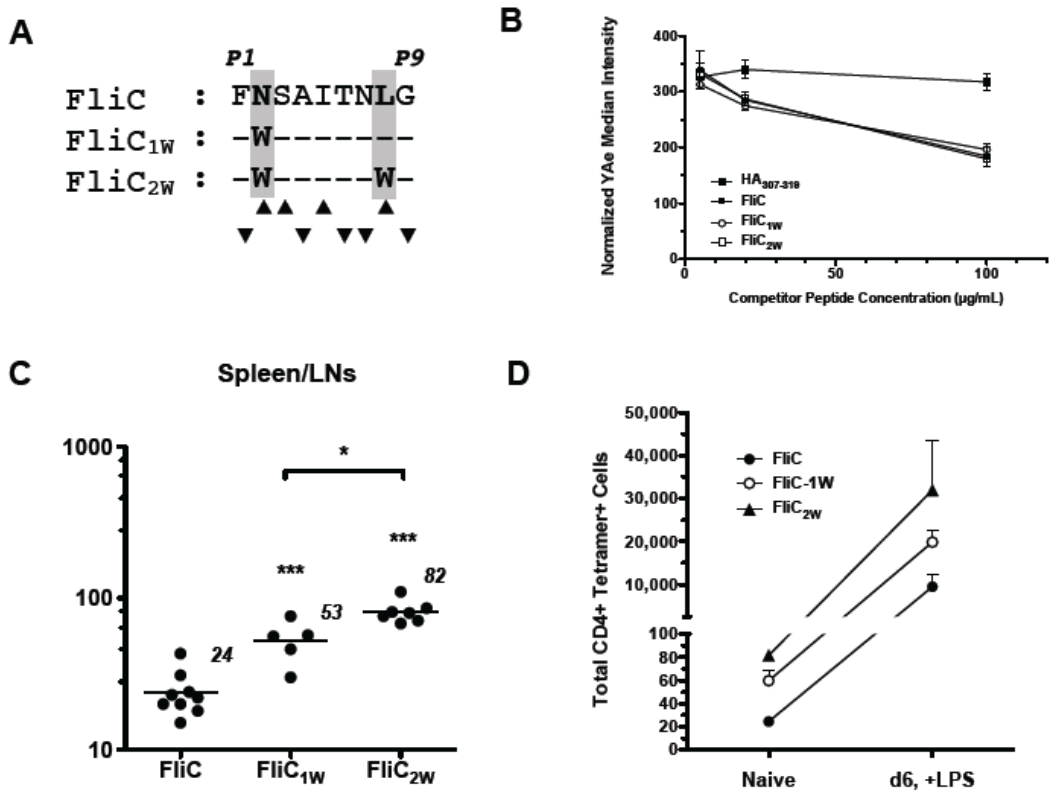

Figure 17. Tryptophan residues at TCR contact P2 and P8 increase FliC:I-A^b-specific T cell population size. A, The core 9 residues of I-A^b-binding peptide FliC and its variants $FliC_{1W}$ and $FliC_{2W}$. The tryptophan residues and their substitutions at P2 and P8 are highlighted. Respective TCR and MHC contact residues are shown. **B,** Normalized median fluorescence intensities of anti-Ea_{52-68}:I-A^b (YAe) staining from B220+ *H2-DMa-/-* spleen after incubation with the Ea_{52-68} peptide plus the indicated concentrations of the control $HA_{307-319}$ peptide or FliC variant peptides. $HA_{307-319}$ (black square), FliC (black circle), $FliC_{1W}$ (open circle), $FliC_{2W}$ (open square). A reduction in Y-Ae staining indicated that the test peptide out competed the Ea_{52-68} peptide for binding to I-A^b. **C,** Total CD3+ CD4+ FliC:I-A^b+, $FliC_{1W}$:I-A^b+ and $FliC_{2W}$:I-A^b+ cells from spleen and all lymph nodes samples of individual B6 mice. Mean values for each group are indicated as horizontal bars and numerically under each set of values. **D,** Mean CD3+ CD4+ FliC:I-A^b+, $FliC_{1W}$:I-A^b+ and $FliC_{2W}$:I-A^b+ cells (± SEM, n = 3-5) from spleen and all lymph nodes samples of individual B6 mice 6 days after i.v. injection with 50 µg of the relevant peptide plus 5 µg LPS. ***, P-value < 0.001; *, P-value < 0.05. Data are representative of at least 3 independent experiments.

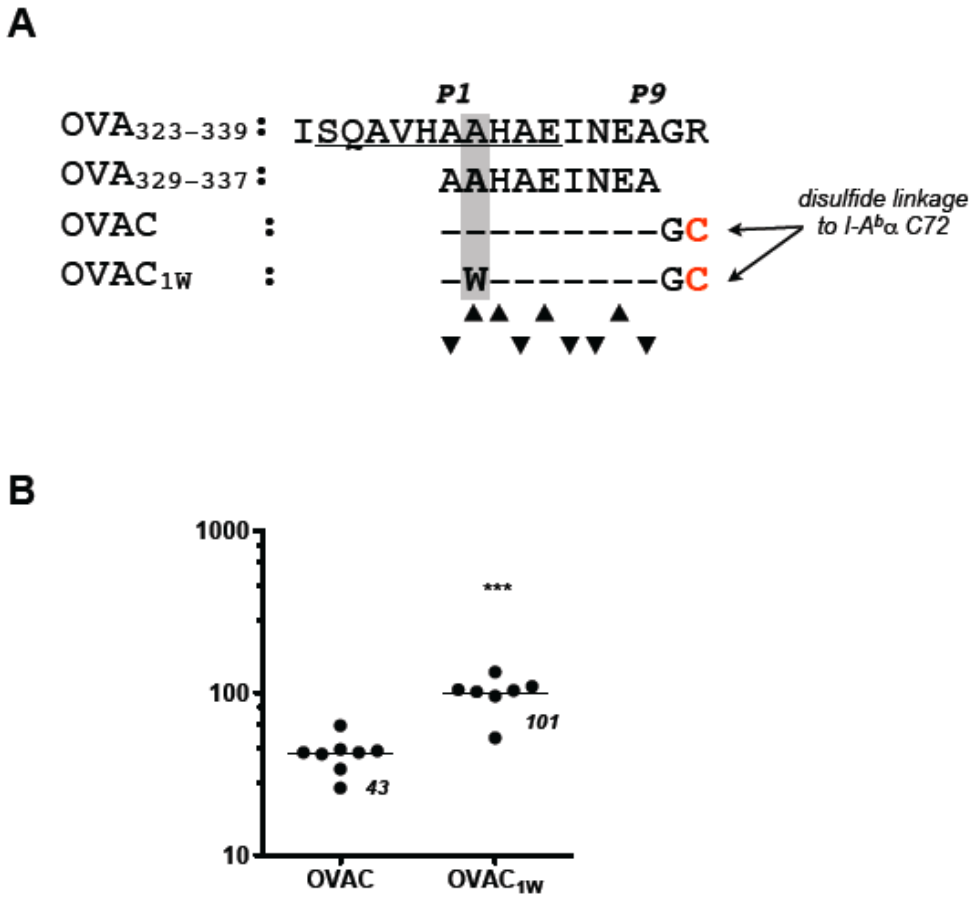

Figure 18. Tryptophan residues at TCR contact P2 increase OVAC:I-A^b-specific T cell population size. A, Residues of I-A^b-binding peptide OVA$_{323-339}$, OVA$_{327-339}$, OVA3C and OVA3C$_{1W}$. The tryptophan residues and their substitutions at P2 and P8 are highlighted. Respective TCR and MHC contact residues are shown. The cysteine residues at the C termini of OVA3C and OVA3C$_{1W}$ for disulfide linkage with the cysteine residues at position 72 of the I-A^b alpha chain are highlighted in red. A second putative I-A^b binding register of OVA$_{323-339}$ is underlined. **B,** Total CD3+ CD4+ OVA3C:I-A^b+ and OVA3C$_{1W}$:I-A^b+ cells from spleen and all lymph nodes samples of individual B6 mice. Mean values for each group are indicated as horizontal bars and numerically under each set of values. ***, *P*-value < 0.001. Data are representative of at least 3 independent experiments.

CHAPTER 5

Summary

This thesis described a novel method that made it possible to analyze the composition of the pre-immune T cell repertoire and the mechanism of immunodominance. These studies have clearly demonstrated that the size of different pMHC-specific CD4+ T cell populations varies. The magnitude and kinetics of the primary immune response of the pMHC-specific populations were shown to be directly proportional to their numbers in the pre-immune repertoire. This phenomenon was confirmed in the CD8+ T cell compartment by other investigators (128-130). Preliminary evidence by screening the TCR Vβ usage of individual pMHC-specific populations suggests that the bigger populations contain more clones instead of more copies of each clone. These observations lead to a major question of how the size hierarchy among the pMHC-specific populations is achieved.

The diverse TCR Vβ usage in the bigger populations suggested that thymic positive selection environment might be more favorable for the TCRs in the bigger populations than those in the smaller ones. Or TCRs in the bigger population might be less susceptible to thymic negative selection because fewer TCRs were cross-reactive to self-pMHC. However, several independent pieces of evidence ruled out these possibilities. First, the size hierarchy of among large and small populations was maintained in mice with severely limited positive or negative selection. Second, the size hierarchy among poplation specific for $pMHC^{A}$ ligands was maintained in mice or humans containing T cell repertoires that were selected on other MHCII molecules.

An alternative possibility was that the pMHC that are recognized by large naïve populations contain special features that contribute to the binding of more TCRs. By comparing the size of populations specific for a series of pMHC variants, we found that peptides containing tryptophan at

the P2 and P8 TCR contact positions were recognized by relatively large naïve populations. Therefore, something about the chemistry of tryptophan gives an advantage over other amino acids for TCR binding. It would be of interest to test whether tyrosine and phenylalanine, which also contain an aromatic ring sidechain, provide similar benefits to any pMHC-specific population.

This thesis provides potentially valuable information for the design for vaccines. Our studies suggest that the primary response originated from a pMHC-specific population of small size may be suboptimal and this population may be more susceptible to extinction due to aging. It could explain why certain individuals fail in responding to vaccination. Using microbial proteins containing immunodominant peptides as the basis of the subunit vaccines may improve their efficacies by targeting naïve T cell populations of larger sizes.

Identification of these peptides from hundreds of proteins from a pathogen will be challenging. Combining information about protein expression patterns, properties and spacing of the MHC-binding residues and residues that are likely to be recognized relative large naïve T cell populations, may make it possible to search for these peptides based on the genome sequence of a pathogen using bioinformatics.

REFERENCES

1. Jenner E, Pasteur L. 1985. [From Jenner to Pasteur or the development of ideas on vaccination]. *Bull Acad Natl Med* 169: 771-8

2. von Behring E, Kitasato S. 1991. [The mechanism of diphtheria immunity and tetanus immunity in animals. 1890]. *Mol Immunol* 28: 1317, 9-20

3. Ehrlich PH, Matsueda GR, Margolies MN, Haber E. 1978. Preparation of an active Fd fragment by cyanogen bromide cleavage of an IgG heavy chain from a homogeneous rabbit antibody. *Immunochemistry* 15: 937-40

4. Witebsky E. 1954. Ehrlich's side-chain theory in the light of present immunology. *Ann N Y Acad Sci* 59: 168-81

5. Jerne NK. 1955. The Natural-Selection Theory of Antibody Formation. *Proc Natl Acad Sci U S A* 41: 849-57

6. Burnet F. 1959. The Clonal Selection Theory. *Cambridge University Press, London*

7. Gowans JL, Mc GD, Cowen DM. 1962. Initiation of immune responses by small lymphocytes. *Nature* 196: 651-5

8. Cooper MD, Peterson RD, Good RA. 1965. Delineation of the Thymic and Bursal Lymphoid Systems in the Chicken. *Nature* 205: 143-6

9. Cooper MD, Raymond DA, Peterson RD, South MA, Good RA. 1966. The functions of the thymus system and the bursa system in the chicken. *J Exp Med* 123: 75-102

10. Katz DH, Hamaoka T, Dorf ME, Maurer PH, Benacerraf B. 1973. Cell interactions between histoincompatible T and B lymphocytes. IV. Involvement of the immune response (Ir) gene in the control of lymphocyte interactions in responses controlled by the gene. *J Exp Med* 138: 734-9

11. Rosenthal AS, Shevach EM. 1973. Function of macrophages in antigen recognition by guinea pig T lymphocytes. I. Requirement for histocompatible macrophages and lymphocytes. *J Exp Med* 138: 1194-212

12. Tonegawa S, Steinberg C, Dube S, Bernardini A. 1974. Evidence for somatic generation of antibody diversity. *Proc Natl Acad Sci U S A* 71: 4027-31

13. Schatz DG, Oettinger MA, Baltimore D. 1989. The V(D)J recombination activating gene, RAG-1. *Cell* 59: 1035-48

14. Davis MM, Bjorkman PJ. 1988. T-cell antigen receptor genes and T-cell recognition. *Nature* 334: 395-402

15. Benacerraf B, McDevitt HO. 1972. Histocompatibility-linked immune response genes. *Science* 175: 273-9

16. Zinkernagel RM, Doherty PC. 1974. Characteristics of the interaction in vitro between cytotoxic thymus- derived lymphocytes and target monolayers infected with lymphocytic choriomeningitis virus. *Scand. J. Immunol.* 3: 287-94

17. Babbitt BP, Allen PM, Matsueda G, Haber E, Unanue ER. 1985. Binding of immunogenic peptides to Ia histocompatibility molecules. *Nature* 317: 359-61

18. Bjorkman PJ, Saper MA, Samraoui B, Bennett WS, Strominger JL, Wiley DC. 1987. Structure of the human class I histocompatibility antigen, HLA-A2. *Nature* 329: 506-12

19. Bjorkman PJ, Saper MA, Samraoui B, Bennett WS, Strominger JL, Wiley DC. 1987. The foreign antigen binding site and T cell recognition regions of class I histocompatibility antigens. *Nature* 329: 512-8

20. Cantor H, Boyse EA. 1975. Functional subclasses of T-lymphocytes bearing different Ly antigens. I. The generation of functionally distinct T-cell subclasses is a differentiative process independent of antigen. *J Exp Med* 141: 1376-89

21. Germain RN. 1994. MHC-dependent antigen processing and peptide presentation: providing ligands for T lymphocyte activation. *Cell* 76: 287-99

22. Moore MW, Carbone FR, Bevan MJ. 1988. Introduction of soluble protein into the class I pathway of antigen processing and presentation. *Cell* 54: 777-85.

23. Paludan C, Schmid D, Landthaler M, Vockerodt M, Kube D, Tuschl T, Munz C. 2005. Endogenous MHC class II processing of a viral nuclear antigen after autophagy. *Science* 307: 593-6

24. Rudolph MG, Stanfield RL, Wilson IA. 2006. How TCRs bind MHCs, peptides, and coreceptors. *Annu. Rev. Immunol.* 24: 419-66

25. Garboczi DN, Ghosh P, Utz U, Fan QR, Biddison WE, Wiley DC. 1996. Structure of the complex between human T-cell receptor, viral peptide and HLA-A2. *Nature* 384: 134-41

26. Garcia KC, Degano M, Stanfield RL, Brunmark A, Jackson MR, Peterson PA, Teyton L, Wilson IA. 1996. An alphabeta T cell receptor structure at 2.5 A and its orientation in the TCR-MHC complex. *Science* 274: 209-19

27. Marrack P, Scott-Browne JP, Dai S, Gapin L, Kappler JW. 2008. Evolutionarily conserved amino acids that control TCR-MHC interaction. *Annu Rev Immunol* 26: 171-203

28. Wallace VA, Penninger J, Mak TW. 1993. CD4, CD8 and tyrosine kinases in thymic selection. *Curr Opin Immunol* 5: 235-40

29. Grusby MJ, Auchincloss H, Jr., Lee R, Johnson RS, Spencer JP, Zijlstra M, Jaenisch R, Papaioannou VE, Glimcher LH. 1993. Mice lacking major histocompatibility complex class I and class II molecules. *Proc. Natl. Acad. Sci. U S A* 90: 3913-7

30. Starr TK, Jameson SC, Hogquist KA. 2003. Positive and negative selection of T cells. *Annu Rev Immunol* 21: 139-76

31. Bevan MJ. 1977. In a radiation chimaera, host H-2 antigens determine immune responsiveness of donor cytotoxic cells. *Nature* 269: 417-8

32. Hogquist KA, Jameson SC, Heath WR, Howard JL, Bevan MJ, Carbone FR. 1994. T cell receptor antagonist peptides induce positive selection. *Cell* 76: 17-27.

33. Alam SM, Travers PJ, Wung JL, Nasholds W, Redpath S, Jameson SC, Gascoigne NR. 1996. T-cell-receptor affinity and thymocyte positive selection. *Nature* 381: 616-20

34. Hogquist KA, Tomlinson AJ, Kieper WC, McGargill MA, Hart MC, Naylor S, Jameson SC. 1997. Identification of a naturally occurring ligand for thymic positive selection. *Immunity* 6: 389-99

35. Lo WL, Felix NJ, Walters JJ, Rohrs H, Gross ML, Allen PM. 2009. An endogenous peptide positively selects and augments the activation and survival of peripheral CD4+ T cells. *Nat Immunol* 10: 1155-61

36. Ebert PJ, Jiang S, Xie J, Li QJ, Davis MM. 2009. An endogenous positively selecting peptide enhances mature T cell responses and becomes an autoantigen in the absence of microRNA miR-181a. *Nat Immunol* 10: 1162-9

37. Singer A, Adoro S, Park JH. 2008. Lineage fate and intense debate: myths, models and mechanisms of CD4- versus CD8-lineage choice. *Nat Rev Immunol* 8: 788-801

38. Taniuchi I, Osato M, Egawa T, Sunshine MJ, Bae SC, Komori T, Ito Y, Littman DR. 2002. Differential requirements for Runx proteins in CD4 repression and epigenetic silencing during T lymphocyte development. *Cell* 111: 621-33

39. He X, Dave VP, Zhang Y, Hua X, Nicolas E, Xu W, Roe BA, Kappes DJ. 2005. The zinc finger transcription factor Th-POK regulates CD4 versus CD8 T-cell lineage commitment. *Nature* 433: 826-33

40. Sun G, Liu X, Mercado P, Jenkinson SR, Kypriotou M, Feigenbaum L, Galera P, Bosselut R. 2005. The zinc finger protein cKrox directs CD4 lineage differentiation during intrathymic T cell positive selection. *Nat Immunol* 6: 373-81

41. McCaughtry TM, Wilken MS, Hogquist KA. 2007. Thymic emigration revisited. *J Exp Med* 204: 2513-20

42. Le Borgne M, Ladi E, Dzhagalov I, Herzmark P, Liao YF, Chakraborty AK, Robey EA. 2009. The impact of negative selection on thymocyte migration in the medulla. *Nat Immunol* 10: 823-30

43. Anderson MS, Venanzi ES, Klein L, Chen Z, Berzins SP, Turley SJ, von Boehmer H, Bronson R, Dierich A, Benoist C, Mathis D. 2002. Projection of an immunological self shadow within the thymus by the aire protein. *Science* 298: 1395-401

44. Derbinski J, Schulte A, Kyewski B, Klein L. 2001. Promiscuous gene expression in medullary thymic epithelial cells mirrors the peripheral self. *Nat Immunol* 2: 1032-9

45. Koble C, Kyewski B. 2009. The thymic medulla: a unique microenvironment for intercellular self-antigen transfer. *J Exp Med* 206: 1505-13

46. Huseby ES, White J, Crawford F, Vass T, Becker D, Pinilla C, Marrack P, Kappler JW. 2005. How the T cell repertoire becomes peptide and MHC specific. *Cell* 122: 247-60

47. Kim JM, Rasmussen JP, Rudensky AY. 2007. Regulatory T cells prevent catastrophic autoimmunity throughout the lifespan of mice. *Nat Immunol* 8: 191-7

48. Zehn D, Bevan MJ. 2006. T cells with low avidity for a tissue-restricted antigen routinely evade central and peripheral tolerance and cause autoimmunity. *Immunity* 25: 261-70

49. Gronski MA, Boulter JM, Moskophidis D, Nguyen LT, Holmberg K, Elford AR, Deenick EK, Kim HO, Penninger JM, Odermatt B, Gallimore A, Gascoigne NR, Ohashi PS. 2004. TCR affinity and negative regulation limit autoimmunity. *Nat Med* 10: 1234-9

50. Medzhitov R, Janeway C, Jr. 2000. Innate immune recognition: mechanisms and pathways. *Immunol. Rev.* 173: 89-97

51. Itano AA, Jenkins MK. 2003. Antigen presentation to naive CD4 T cells in the lymph node. *Nat. Immunol.* 4: 733-9

52. Itano AA, McSorley SJ, Reinhardt RL, Ehst BD, Ingulli E, Rudensky AY, Jenkins MK. 2003. Distinct dendritic cell populations sequentially

present antigen to CD4 T cells and stimulate different aspects of cell-mediated immunity. *Immunity* 19: 47-57

53. Chtanova T, Han SJ, Schaeffer M, van Dooren GG, Herzmark P, Striepen B, Robey EA. 2009. Dynamics of T cell, antigen-presenting cell, and pathogen interactions during recall responses in the lymph node. *Immunity* 31: 342-55

54. Mempel TR, Henrickson SE, Von Andrian UH. 2004. T-cell priming by dendritic cells in lymph nodes occurs in three distinct phases. *Nature* 427: 154-9

55. Jenkins MK, Khoruts A, Ingulli E, Mueller DL, McSorley SJ, Reinhardt RL, Itano A, Pape KA. 2001. In vivo activation of antigen-specific CD4 T cells. *Annu. Rev. Immunol.* 19: 23-45

56. Reis e Sousa C. 2004. Toll-like receptors and dendritic cells: for whom the bug tolls. *Semin Immunol* 16: 27-34

57. DeSilva DR, Urdahl KB, Jenkins MK. 1991. Clonal anergy is induced in vitro by T cell receptor occupancy in the absence of proliferation. *J. Immunol.* 147: 3261-7

58. Kearney ER, Pape KA, Loh DY, Jenkins MK. 1994. Visualization of peptide-specific T cell immunity and peripheral tolerance induction in vivo. *Immunity* 1: 327-39

59. Schwartz RH. 2003. T cell anergy. *Annu. Rev. Immunol.* 21: 305-34

60. Malherbe L, Hausl C, Teyton L, McHeyzer-Williams MG. 2004. Clonal selection of helper T cells is determined by an affinity threshold with no further skewing of TCR binding properties. *Immunity* 21: 669-79

61. Zehn D, Lee SY, Bevan MJ. 2009. Complete but curtailed T-cell response to very low-affinity antigen. *Nature* 458: 211-4

62. Teixeiro E, Daniels MA, Hamilton SE, Schrum AG, Bragado R, Jameson SC, Palmer E. 2009. Different T cell receptor signals determine CD8+ memory versus effector development. *Science* 323: 502-5

63. Fazilleau N, McHeyzer-Williams LJ, Rosen H, McHeyzer-Williams MG. 2009. The function of follicular helper T cells is regulated by the strength of T cell antigen receptor binding. *Nat Immunol* 10: 375-84

64. Zhu J, Paul WE. 2008. CD4 T cells: fates, functions, and faults. *Blood* 112: 1557-69

65. Hosken NA, Shibuya K, Heath AW, Murphy KM, O'Garra A. 1995. The effect of antigen dose on CD4+ T helper cell phenotype development in a T cell receptor-alpha beta-transgenic model. *J Exp Med* 182: 1579-84

66. Mullen AC, High FA, Hutchins AS, Lee HW, Villarino AV, Livingston DM, Kung AL, Cereb N, Yao T-P, Yang SY, Reiner SL. 2001. Role of T-bet in committment of Th1 cells before IL-12-dependent selection. *Science* 292: 1907-10

67. Hsieh CS, Heimberger AB, Gold JS, O'Garra A. 1992. Development of Th1 CD4+ T cells through IL-12 produced by *Listeria*-induced macrophages. *Science* 260: 547-9

68. Reiner SL, Locksley RM. 1995. The regulation of immunity to Leishmania major. *Annu. Rev. Immunol.* 13: 151-77

69. Beal AM, Anikeeva N, Varma R, Cameron TO, Vasiliver-Shamis G, Norris PJ, Dustin ML, Sykulev Y. 2009. Kinetics of early T cell receptor signaling regulate the pathway of lytic granule delivery to the secretory domain. *Immunity* 31: 632-42

70. Jenkins MR, Tsun A, Stinchcombe JC, Griffiths GM. 2009. The strength of T cell receptor signal controls the polarization of cytotoxic machinery to the immunological synapse. *Immunity* 31: 621-31

71. Yewdell JW. 2006. Confronting complexity: real-world immunodominance in antiviral CD8+ T cell responses. *Immunity* 25: 533-43

72. Yewdell JW, Bennink JR. 1999. Immunodominance in major histocompatibility complex class I-restricted T lymphocyte responses. *Annu Rev Immunol* 17: 51-88

73. Corradin G, Etlinger HM, Chiller JM. 1977. Lymphocyte specificity to protein antigens. I. Characterization of the antigen-induced in vitro T cell-dependent proliferative response with lymph node cells from primed mice. *J Immunol* 119: 1048-53

74. Jenkins MK, Melvold RW, Miller SD. 1984. Isolation and characterization of an I-A-restricted T cell clone with dual specificity for poly(Glu60Ala30Tyr10) (GAT) and Mlsa,dl. *J. Immunol.* 133: 616-22

75. Steinmetz M, Bluthmann H, Ryser S, Uematsu Y. 1989. Transgenic mice to study T-cell receptor gene regulation and repertoire formation. *Genome* 31: 652-5

76. Pape KA, Kearney ER, Khoruts A, Mondino A, Merica R, Chen ZM, Ingulli E, White J, Johnson JG, Jenkins MK. 1997. Use of adoptive transfer of T-cell-antigen-receptor-transgenic T cell for the study of T-cell activation in vivo. *Immunol. Rev.* 156: 67-78.

77. Marzo AL, Klonowski KD, Le Bon A, Borrow P, Tough DF, Lefrancois L. 2005. Initial T cell frequency dictates memory CD8+ T cell lineage commitment. *Nat Immunol* 6: 793-9

78. Hataye J, Moon JJ, Khoruts A, Reilly C, Jenkins MK. 2006. Naive and memory CD4+ T cell survival controlled by clonal abundance. *Science* 312: 114-6

79. Moon JJ, Chu HH, Hataye J, Pagan AJ, Pepper M, McLachlan JB, Zell T, Jenkins MK. 2009. Tracking epitope-specific T cells. *Nat Protoc* 4: 565-81

80. Altman JD, Moss PA, Goulder PJ, Barouch DH, McHeyzer-Williams MG, Bell JI, McMichael AJ, Davis MM. 1996. Phenotypic analysis of antigen-specific T lymphocytes. *Science* 274: 94-6.

81. Crawford F, Kozono H, White J, Marrack P, Kappler J. 1998. Detection of antigen-specific T cells with multivalent soluble class II MHC covalent peptide complexes. *Immunity* 8: 675-82

82. Malherbe L, Filippi C, Julia V, Foucras G, Moro M, Appel H, Wucherpfennig K, Guery JC, Glaichenhaus N. 2000. Selective

activation and expansion of high-affinity CD4+ T cells in resistant mice upon infection with Leishmania major. *Immunity* 13: 771-82

83. Scott CA, Garcia KC, Carbone FR, Wilson IA, Teyton L. 1996. Role of chain pairing for the production of functional soluble IA major histocompatibility complex class II molecules. *J Exp Med* 183: 2087-95

84. Beckett D, Kovaleva E, Schatz PJ. 1999. A minimal peptide substrate in biotin holoenzyme synthetase-catalyzed biotinylation. *Protein Sci.* 8: 921-9

85. Kozono H, White J, Clements J, Marrack P, Kappler J. 1994. Production of soluble MHC class II proteins with covalently bound single peptides. *Nature* 369: 151-4

86. Wedderburn LR, Searle SJ, Rees AR, Lamb JR, Owen MJ. 1995. Mapping T cell recognition: the identification of a T cell receptor residue critical to the specific interaction with an influenza hemagglutinin peptide. *Eur J Immunol* 25: 1654-62

87. Ignatowicz L, Rees W, Pacholczyk R, Ignatowicz H, Kushnir E, Kappler J, Marrack P. 1997. T cells can be activated by peptides that are unrelated in sequence to their selecting peptide. *Immunity* 7: 179-86

88. Murphy DB, Lo D, Rath S, Brinster RL, Flavell RA, Slanetz A, Janeway CA, Jr. 1989. A novel MHC class II epitope expressed in thymic medulla but not cortex. *Nature* 338: 765-8

89. Rudensky A, Rath S, Preston-Hurlburt P, Murphy DB, Janeway CA, Jr. 1991. On the complexity of self. *Nature* 353: 660-2.

90. Stockinger B, Bourgeois C, Kassiotis G. 2006. CD4+ memory T cells: functional differentiation and homeostasis. *Immunol. Rev.* 211: 39-48

91. Busch DH, Pilip IM, Vijh S, Pamer EG. 1998. Coordinate regulation of complex T cell populations responding to bacterial infection. *Immunity* 8: 353-62

92. Homann D, Teyton L, Oldstone MB. 2001. Differential regulation of antiviral T-cell immunity results in stable CD8+ but declining CD4+ T-cell memory. *Nat. Med.* 7: 913-9.

93. McHeyzer-Williams MG, Davis MM. 1995. Antigen-specific development of primary and memory T cells in vivo. *Science* 268: 106-11

94. Blattman JN, Antia R, Sourdive DJ, Wang X, Kaech SM, Murali-Krishna K, Altman JD, Ahmed R. 2002. Estimating the precursor frequency of naive antigen-specific CD8 T cells. *J. Exp. Med.* 195: 657-64.

95. Butz EA, Bevan MJ. 1998. Massive expansion of antigen-specific CD8+ T cells during an acute virus infection. *Immunity* 8: 167-75

96. Stetson DB, Mohrs M, Mallet-Designe V, Teyton L, Locksley RM. 2002. Rapid expansion and IL-4 expression by Leishmania-specific naive helper T cells in vivo. *Immunity* 17: 191-200

97. Whitmire JK, Benning N, Whitton JL. 2006. Precursor frequency, nonlinear proliferation, and functional maturation of virus-specific CD4+ T cells. *J Immunol* 176: 3028-36

98. Badovinac VP, Haring JS, Harty JT. 2007. Initial T cell receptor transgenic cell precursor frequency dictates critical aspects of the CD8(+) T cell response to infection. *Immunity* 179: 53-63

99. Ford ML, Koehn BH, Wagener ME, Jiang W, Gangappa S, Pearson TC, Larsen CP. 2007. Antigen-specific precursor frequency impacts T cell proliferation, differentiation, and requirement for costimulation. *J Exp Med* 204: 299-309

100. Foulds KE, Shen H. 2006. Clonal competition inhibits the proliferation and differentiation of adoptively transferred TCR transgenic CD4 T cells in response to infection. *J Immunol* 176: 3037-43

101. Rees W, Bender J, Teague TK, Kedl RM, Crawford F, Marrack P, Kappler J. 1999. An inverse relationship between T cell receptor affinity and antigen dose during CD4(+) T cell responses in vivo and in vitro. *Proc. Natl. Acad. Sci. U S A* 96: 9781-6.

102. Rudensky A, Preston-Hurlburt P, Hong SC, Barlow A, Janeway CA, Jr. 1991. Sequence analysis of peptides bound to MHC class II molecules. *Nature* 353: 622-7

103. McSorley SJ, Cookson BT, Jenkins MK. 2000. Characterization of CD4+ T cell responses during natural infection with Salmonella typhimurium. *J. Immunol.* 164: 986-93.

104. Shimonkevitz R, Colon S, Kappler JW, Marrack P, Grey HM. 1984. Antigen recognition by H-2-restricted T cells. II. A tryptic ovalbumin peptide that substitutes for processed antigen. *J. Immunol.* 133: 2067-74

105. Dutton RW, Bradley LM, Swain SL. 1998. T cell memory. *Annu. Rev. Immunol.* 16: 201-23

106. McSorley SJ, Asch S, Costalonga M, Reinhardt RL, Jenkins MK. 2002. Tracking Salmonella-specific CD4 T cells in vivo reveals a local mucosal response to a disseminated infection. *Immunity* 16: 71-83

107. Barnden MJ, Allison J, Heath WR, Carbone FR. 1998. Defective TCR expression in transgenic mice constructed using cDNA-based alpha- and beta-chain genes under the control of heterologous regulatory elements. *Immunol. Cell. Biol.* 76: 34-40

108. Pearce EL, Shedlock DJ, Shen H. 2004. Functional characterization of MHC class II-restricted CD8+CD4- and CD8-CD4- T cell responses to infection in CD4-/- mice. *J Immunol* 173: 2494-9

109. Tyznik AJ, Sun JC, Bevan MJ. 2004. The CD8 population in CD4-deficient mice is heavily contaminated with MHC class II-restricted T cells. *J. Exp. Med.* 199: 559-65

110. Klinman NR. 1972. The mechanism of antigenic stimulation of primary and secondary clonal precursor cells. *J Exp Med* 136: 241-60

111. Felix NJ, Donermeyer DL, Horvath S, Walters JJ, Gross ML, Suri A, Allen PM. 2007. Alloreactive T cells respond specifically to multiple distinct peptide-MHC complexes. *Nat. Immunol.* 8: 388-97

112. Evavold BD, Sloan-Lancaster J, Wilson KJ, Rothbard JB, Allen PM. 1995. Specific T cell recognition of minimally homologous peptides: evidence for multiple endogenous ligands. *Immunity* 2: 655-63

113. Casrouge A, Beaudoing E, Dalle S, Pannetier C, Kanellopoulos J, Kourilsky P. 2000. Size estimate of the alpha beta TCR repertoire of naive mouse splenocytes. *J. Immunol.* 164: 5782-7

114. Kedzierska K, Day EB, Pi J, Heard SB, Doherty PC, Turner SJ, Perlman S. 2006. Quantification of repertoire diversity of influenza-specific epitopes with predominant public or private TCR usage. *J Immunol* 177: 6705-12

115. Masopust D, Murali-Krishna K, Ahmed R. 2007. Quantitating the magnitude of the lymphocytic choriomeningitis virus-specific CD8 T-cell response: it is even bigger than we thought. *J Virol*. 81: 2002-11

116. Boursalian TE, Golob J, Soper DM, Cooper CJ, Fink PJ. 2004. Continued maturation of thymic emigrants in the periphery. *Nat. Immunol.* 5: 418-25

117. Kaech SM, Ahmed R. 2001. Memory CD8+ T cell differentiation: initial antigen encounter triggers a developmental program in naive cells. *Nat Immunol* 2: 415-22

118. Mercado R, Vijh S, Allen SE, Kerksiek K, Pilip IM, Pamer EG. 2000. Early programming of T cell populations responding to bacterial infection. *J Immunol* 165: 6833-9

119. van Stipdonk MJ, Lemmens EE, Schoenberger SP. 2001. Naive CTLs require a single brief period of antigenic stimulation for clonal expansion and differentiation. *Nat Immunol* 2: 423-9

120. Obst R, van Santen HM, Mathis D, Benoist C. 2005. Antigen persistence is required throughout the expansion phase of a CD4(+) T cell response. *J. Exp. Med.* 201: 1555-65

121. Bousso P, Casrouge A, Altman JD, Haury M, Kanellopoulos J, Abastado JP, Kourilsky P. 1998. Individual variations in the murine T cell response to a specific peptide reflect variability in naive repertoires. *Immunity* 9: 169-78

122. Prlic M, Jameson SC. 2002. Homeostatic expansion versus antigen-driven proliferation: common ends by different means? *Microbes Infect* 4: 531-7
123. Davis MM, Boniface JJ, Reich Z, Lyons D, Hampl J, Arden B, Chien Y. 1998. Ligand recognition by alpha beta T cell receptors. *Annu. Rev. Immunol.* 16: 523-44

124. Hogquist KA, Baldwin TA, Jameson SC. 2005. Central tolerance: learning self-control in the thymus. *Nat. Rev. Immunol.* 5: 772-82

125. Sprent J. 1978. Restricted helper function of F1 leads to parent bone marrow chimeras controlled by K-end of H-2 complex. *J Exp Med* 147: 1838-42

126. Berg LJ, Davis MM. 1989. T-cell development in T cell receptor alphabeta transgenic mice. *Semin Immunol* 1: 105-16

127. Moon JJ, Chu HH, Pepper M, McSorley SJ, Jameson SC, Kedl RM, Jenkins MK. 2007. Naive CD4(+) T cell frequency varies for different epitopes and predicts repertoire diversity and response magnitude. *Immunity* 27: 203-13

128. Obar JJ, Khanna KM, Lefrancois L. 2008. Endogenous naive CD8+ T cell precursor frequency regulates primary and memory responses to infection. *Immunity* 28: 859-69

129. Kotturi MF, Scott I, Wolfe T, Peters B, Sidney J, Cheroutre H, von Herrath MG, Buchmeier MJ, Grey H, Sette A. 2008. Naive precursor frequencies and MHC binding rather than the degree of epitope diversity shape CD8+ T cell immunodominance. *J Immunol* 181: 2124-33

130. Haluszczak C, Akue AD, Hamilton SE, Johnson LD, Pujanauski L, Teodorovic L, Jameson SC, Kedl RM. 2009. The antigen-specific CD8+ T cell repertoire in unimmunized mice includes memory phenotype cells bearing markers of homeostatic expansion. *J Exp Med* 206: 435-48

131. Murphy DB, Rath S, Pizzo E, Rudensky AY, George A, Larson JK, Janeway CA, Jr. 1992. Monoclonal antibody detection of a major self peptide. MHC class II complex. *J. Immunol.* 148: 3483-91

132. Matzinger P, Guerder S. 1989. Does T-cell tolerance require a dedicated antigen-presenting cell? *Nature* 338: 74-6

133. Vukmanovic S, Grandea AG, 3rd, Faas SJ, Knowles BB, Bevan MJ. 1992. Positive selection of T-lymphocytes induced by intrathymic injection of a thymic epithelial cell line. *Nature* 359: 729-32

134. Vasquez NJ, Kaye J, Hedrick SM. 1992. In vivo and in vitro clonal deletion of double-positive thymocytes. *J Exp Med* 175: 1307-16

135. Markowitz JS, Auchincloss H, Jr., Grusby MJ, Glimcher LH. 1993. Class II-positive hematopoietic cells cannot mediate positive selection of CD4+ T lymphocytes in class II-deficient mice. *Proc Natl Acad Sci U S A* 90: 2779-83

136. Chu HH, Moon JJ, Takada K, Pepper M, Molitor JA, Schacker TW, Hogquist KA, Jameson SC, Jenkins MK. 2009. Positive selection optimizes the number and function of MHCII-restricted CD4+ T cell clones in the naive polyclonal repertoire. *Proc Natl Acad Sci U S A* 106: 11241-5

137. Yager EJ, Ahmed M, Lanzer K, Randall TD, Woodland DL, Blackman MA. 2008. Age-associated decline in T cell repertoire diversity leads to holes in the repertoire and impaired immunity to influenza virus. *J Exp Med* 205: 711-23

138. Ahmed M, Lanzer KG, Yager EJ, Adams PS, Johnson LL, Blackman MA. 2009. Clonal expansions and loss of receptor diversity in the naive CD8 T cell repertoire of aged mice. *J Immunol* 182: 784-92

139. Turner SJ, Kedzierska K, Komodromou H, La Gruta NL, Dunstone MA, Webb AI, Webby R, Walden H, Xie W, McCluskey J, Purcell AW, Rossjohn J, Doherty PC. 2005. Lack of prominent peptide-major histocompatibility complex features limits repertoire diversity in virus-specific CD8+ T cell populations. *Nat Immunol* 6: 382-9

140. Meijers R, Lai CC, Yang Y, Liu JH, Zhong W, Wang JH, Reinherz EL. 2005. Crystal structures of murine MHC Class I H-2 D(b) and K(b) molecules in complex with CTL epitopes from influenza A virus: implications for TCR repertoire selection and immunodominance. *J Mol Biol* 345: 1099-110

141. Kedzierska K, Guillonneau C, Gras S, Hatton LA, Webby R, Purcell AW, Rossjohn J, Doherty PC, Turner SJ. 2008. Complete modification of TCR specificity and repertoire selection does not perturb a CD8+ T cell immunodominance hierarchy. *Proc Natl Acad Sci U S A* 105: 19408-13

142. Stewart-Jones GB, McMichael AJ, Bell JI, Stuart DI, Jones EY. 2003. A structural basis for immunodominant human T cell receptor recognition. *Nat Immunol* 4: 657-63

143. Fung-Leung WP, Surh CD, Liljedahl M, Pang J, Leturcq D, Peterson PA, Webb SR, Karlsson L. 1996. Antigen presentation and T cell development in H2-M-deficient mice. *Science* 271: 1278-81

144. Miyazaki T, Wolf P, Tourne S, Waltzinger C, Dierich A, Barois N, Ploegh H, Benoist C, Mathis D. 1996. Mice lacking H2-M complexes, enigmatic elements of the MHC class II peptide-loading pathway. *Cell* 84: 531-41

145. Martin WD, Hicks GG, Mendiratta SK, Leva HI, Ruley HE, Van Kaer L. 1996. H2-M mutant mice are defective in the peptide loading of class II molecules, antigen presentation, and T cell repertoire selection. *Cell* 84: 543-50

146. Ignatowicz L, Kappler J, Marrack P. 1996. The repertoire of T cells shaped by a single MHC/peptide ligand. *Cell* 84: 521-9

147. Fukui Y, Ishimoto T, Utsuyama M, Gyotoku T, Koga T, Nakao K, Hirokawa K, Katsuki M, Sasazuki T. 1997. Positive and negative CD4+ thymocyte selection by a single MHC class II/peptide ligand affected by its expression level in the thymus. *Immunity* 6: 401-10

148. Surh CD, Lee DS, Fung-Leung WP, Karlsson L, Sprent J. 1997. Thymic selection by a single MHC/peptide ligand produces a semidiverse repertoire of CD4+ T cells. *Immunity* 7: 209-19

149. Viret C, Wong FS, Janeway CA, Jr. 1999. Designing and maintaining the mature TCR repertoire: the continuum of self-peptide:self-MHC complex recognition. *Immunity* 10: 559-68

150. Dongre AR, Kovats S, deRoos P, McCormack AL, Nakagawa T, Paharkova-Vatchkova V, Eng J, Caldwell H, Yates JR, 3rd, Rudensky AY. 2001. In vivo MHC class II presentation of cytosolic proteins revealed by rapid automated tandem mass spectrometry and functional analyses. *Eur J Immunol* 31: 1485-94
151. Bill J, Palmer E. 1989. Positive selection of CD4+ T cells mediated by MHC class II-bearing stromal cell in the thymic cortex. *Nature* 341: 649-51

152. Laufer TM, DeKoning J, Markowitz JS, Lo D, Glimcher LH. 1996. Unopposed positive selection and autoreactivity in mice expressing class II MHC only on thymic cortex. *Nature* 383: 81-5

153. Laufer TM, Fan L, Glimcher LH. 1999. Self-reactive T cells selected on thymic cortical epithelium are polyclonal and are pathogenic in vivo. *J Immunol* 162: 5078-84

154. Zhu Y, Rudensky AY, Corper AL, Teyton L, Wilson IA. 2003. Crystal structure of MHC class II I-Ab in complex with a human CLIP peptide: prediction of an I-Ab peptide-binding motif. *J Mol Biol* 326: 1157-74

155. Liu X, Dai S, Crawford F, Fruge R, Marrack P, Kappler J. 2002. Alternate interactions define the binding of peptides to the MHC molecule IA(b). *Proc Natl Acad Sci U S A* 99: 8820-5

156. Robertson JM, Jensen PE, Evavold BD. 2000. DO11.10 and OT-II T cells recognize a C-terminal ovalbumin 323-339 epitope. *J Immunol* 164: 4706-12

157. Truscott SM, Lybarger L, Martinko JM, Mitaksov VE, Kranz DM, Connolly JM, Fremont DH, Hansen TH. 2007. Disulfide bond engineering to trap peptides in the MHC class I binding groove. *J Immunol* 178: 6280-9

158. Barton GM, Rudensky AY. 1999. Requirement for diverse, low-abundance peptides in positive selection of T cells. *Science* 283: 67-70

159. Gallivan JP, Dougherty DA. 1999. Cation-pi interactions in structural biology. *Proc Natl Acad Sci U S A* 96: 9459-64

160. Chen JL, Stewart-Jones G, Bossi G, Lissin NM, Wooldridge L, Choi EM, Held G, Dunbar PR, Esnouf RM, Sami M, Boulter JM, Rizkallah P, Renner C, Sewell A, van der Merwe PA, Jakobsen BK, Griffiths G, Jones EY, Cerundolo V. 2005. Structural and kinetic basis for heightened immunogenicity of T cell vaccines. *J Exp Med* 201: 1243-55